CHAPTER 7

Methods of Analyzing Slope Stability

Methods for analyzing stability of slopes include simple equations, charts, spreadsheet software, and slope stability computer programs. In many cases more than one method can be used to evaluate the stability for a particular slope. For example, simple equations or charts may be used to make a preliminary estimate of slope stability, and later, a computer program may be used for detailed analyses. Also, if a computer program is used, another computer program, slope stability charts, or a spreadsheet should be used to verify results. The various methods used to compute a factor of safety are presented in this chapter.

SIMPLE METHODS OF ANALYSIS

The simplest methods of analysis employ a single simple algebraic equation to compute the factor of safety. These equations require at most a hand calculator to solve. Such simple equations exist for computing the stability of a vertical slope in purely cohesive soil, of an embankment on a much weaker, deep foundation, and of an infinite slope. Some of these methods, such as the method for computing the stability of an infinite slope, may provide a rigorous solution, whereas others, such as the equations used to estimate the stability of a vertical slope, represent some degree of approximation. Several simple methods are described below.

Vertical Slope in Cohesive Soil

For a vertical slope in cohesive soil a simple expression for the factor of safety is obtained based on a planar slip surface like the one shown in Figure 7.1. The average shear stress, τ, along the slip plane is expressed as

$$\tau = \frac{W \sin \alpha}{l} = \frac{W \sin \alpha}{H/\sin \alpha} = \frac{W \sin^2 \alpha}{H} \tag{7.1}$$

where α is the inclination of the slip plane, H is the slope height, and W is the weight of the soil mass. The weight, W, is expressed as

$$W = \frac{1}{2} \frac{\gamma H^2}{\tan \alpha} \tag{7.2}$$

which when substituted into Eq. (7.2) and rearranged gives

$$\tau = \tfrac{1}{2} \gamma H \sin \alpha \cos \alpha \tag{7.3}$$

For a cohesive soil ($\phi = 0$) the factor of safety is expressed as

$$F = \frac{c}{\tau} = \frac{2c}{\gamma H \sin \alpha \cos \alpha} \tag{7.4}$$

To find the minimum factor of safety, the inclination of the slip plane is varied. The minimum factor of safety is found for $\alpha = 45°$. Substituting this value for α (45°) into Eq. (7.4) gives

$$F = \frac{4c}{\gamma H} \tag{7.5}$$

Equation (7.5) gives the factor of safety for a vertical slope in cohesive soil, assuming a plane slip surface. Circular slip surfaces give a slightly lower value for the factor of safety ($F = 3.83c/\gamma h$); however, the difference between the factors of safety based on a plane and a circular slip surface is small for a vertical slope in cohesive soil and can be ignored.

Copyrighted Material

Copyright © 2005 John Wiley & Sons Retrieved from: www.knovel.com

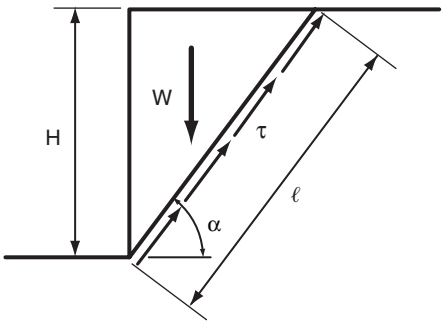


Figure 7.1 Vertical slope and plane slip surface.

Equation (7.5) can also be rearranged to calculate the critical height of a vertical slope (i.e., the height of a slope that has a factor of safety of unity). The critical height of a vertical slope in cohesive soil is

$$H_{\text{critical}} = \frac{4c}{\gamma} \tag{7.6}$$

Bearing Capacity Equations

The equations used to calculate the bearing capacity of foundations can also be used to estimate the stability of embankments on deep deposits of saturated clay. For a saturated clay and undrained loading ($\phi = 0$), the ultimate bearing capacity, q_{ult}, based on a circular slip surface is[1]

$$q_{\text{ult}} = 5.53c \tag{7.7}$$

Equating the ultimate bearing capacity to the load, $q = \gamma H$, produced by an embankment of height, H, gives

$$\gamma H = 5.53c \tag{7.8}$$

where γ is the unit weight of the soil in the embankment; γh represents the maximum vertical stress produced by the embankment. Equation (7.8) is an equilibrium equation corresponding to ultimate conditions (i.e., with the shear strength of the soil fully developed). If, instead, only some fraction of the shear strength is developed (i.e., the factor of safety is greater than unity), a factor of safety can be introduced into the equilibrium equation (7.8) and we can write

$$\gamma H = 5.53 \frac{c}{F} \tag{7.9}$$

In this equation F is the factor of safety with respect to shear strength; the term c/F represents the developed cohesion, c_d. Equation (7.9) can be rearranged to give

$$F = 5.53 \frac{c}{\gamma H} \tag{7.10}$$

Equation (7.10) can be used to estimate the factor of safety against a deep-seated failure of an embankment on soft clay.

Equation (7.10) gives a conservative estimate of the factor of safety of an embankment because it ignores the strength of the embankment and the depth of the foundation in comparison with the embankment width. Alternative bearing capacity equations that are applicable to reinforced embankments on thin clay foundations are presented in Chapter 8.

Infinite Slope

In Chapter 6 the equations for an infinite slope were presented. For these equations to be applicable, the depth of the slip surface must be small compared to the lateral extent of the slope. However, in the case of cohesionless soils, the factor of safety does not depend on the depth of the slip surface. It is possible for a slip surface to form at a small enough depth that the requirements for an infinite slope are met, regardless of the extent of the slope. Therefore, an infinite slope analysis is rigorous and valid for cohesionless slopes. The infinite slope analysis procedure is also applicable to other cases where the slip surface is parallel to the face of the slope and the depth of the slip surface is small compared to the lateral extent of the slope. This condition may exist where there is a stronger layer of soil at shallow depth: for example, where a layer of weathered soil exists near the surface of the slope and is underlain by stronger, unweathered material.

The general equation for the factor of safety for an infinite slope with the shear strength expressed in terms of total stresses is

$$F = \cot \beta \tan \phi + (\cot \beta + \tan \beta) \frac{c}{\gamma z} \tag{7.11}$$

[1] Although Prandtl's solution of $q_{\text{ult}} = 5.14c$ is commonly used for bearing capacity, it is more appropriate to use the solution based on circles, which gives a somewhat higher bearing capacity and offsets some of the inherent conservatism introduced when bearing capacity equations are applied to slope stability.

Copyrighted Material

Copyright © 2005 John Wiley & Sons Retrieved from: www.knovel.com

where z is the vertical depth of the slip surface below the face of the slope. For shear strengths expressed by effective stresses the equation for the factor of safety can be written as

$$F = \left[\cot \beta - \frac{u}{\gamma z}(\cot \beta + \tan \beta)\right] \tan \phi' + (\cot \beta + \tan \beta)\frac{c'}{\gamma z} \quad (7.12)$$

where u is the pore water pressure at the depth of the slip surface.

For effective stress analyses, Eq. (7.12) can also be written as

$$F = [\cot \beta - r_u (\cot \beta + \tan \beta)] \tan \phi' + (\cot \beta + \tan \beta) \frac{c'}{\gamma z} \quad (7.13)$$

where r_u is the pore pressure ratio defined by Bishop and Morgenstern (1960) as

$$r_u = \frac{u}{\gamma z} \quad (7.14)$$

Values of r_u can be determined for specific seepage conditions. For example, for seepage parallel to the slope, the pore pressure ratio, r_u, is given by

$$r_u = \frac{\gamma_w}{\gamma} \frac{h_w}{z} \cos^2\beta \quad (7.15)$$

where h_w is the height of the free water surface vertically above the slip surface (Figure 7.2*a*). If the seepage exits the slope face at an angle (Figure 7.2*b*), the value of r_u is given by

$$r_u = \frac{\gamma_w}{\gamma} \frac{1}{1 + \tan \beta \tan \theta} \quad (7.16)$$

where θ is the angle between the direction of seepage (flow lines) and the horizontal. For the special case of horizontal seepage ($\theta = 0$), the expression for r_u reduces to

$$r_u = \frac{\gamma_w}{\gamma} \quad (7.17)$$

Recapitulation

- Simple equations can be used to compute the factor of safety for several slope and shear strength conditions, including a vertical slope in cohesive soil, an embankment on a deep deposit of saturated clay, and an infinite slope.
- Depending on the particular slope conditions and equations used, the accuracy ranges from excellent, (e.g., for a homogeneous slope in cohesionless soil) to relatively crude (e.g., for bearing capacity of an embankment on saturated clay).

SLOPE STABILITY CHARTS

The stability of many relatively homogeneous slopes can be calculated using slope stability charts based on one of the analysis procedures presented in Chapter 6. Fellenius (1936) was one of the first to recognize that factors of safety could be expressed by charts. His work was followed by the work of Taylor (1937) and Janbu (1954*b*). Since the pioneering work of these authors, numerous others have developed charts for computing the stability of slopes. However, the early charts of Janbu are still some of the most useful for many conditions, and these are described in further detail in the Appendix. The charts cover a range in slope and soil conditions and they are quite easy to use. In addition, the charts provide the minimum factor of safety and eliminate the need to search for a critical slip surface.

Stability charts rely on dimensionless relationships that exist between the factor of safety and other parameters that describe the slope geometry, soil shear strengths, and pore water pressures. For example, the infinite slope equation for effective stresses presented earlier [Eq. (7.13)] can be written as

$$F = [1 - r_u(1 + \tan^2\beta)] \frac{\tan \phi'}{\tan \beta} + (1 + \tan^2\beta) \frac{c'}{\gamma z} \quad (7.18)$$

or

$$F = A \frac{\tan \phi'}{\tan \beta} + B \frac{c'}{\gamma z} \quad (7.19)$$

where

Copyrighted Material

Copyright © 2005 John Wiley & Sons Retrieved from: www.knovel.com

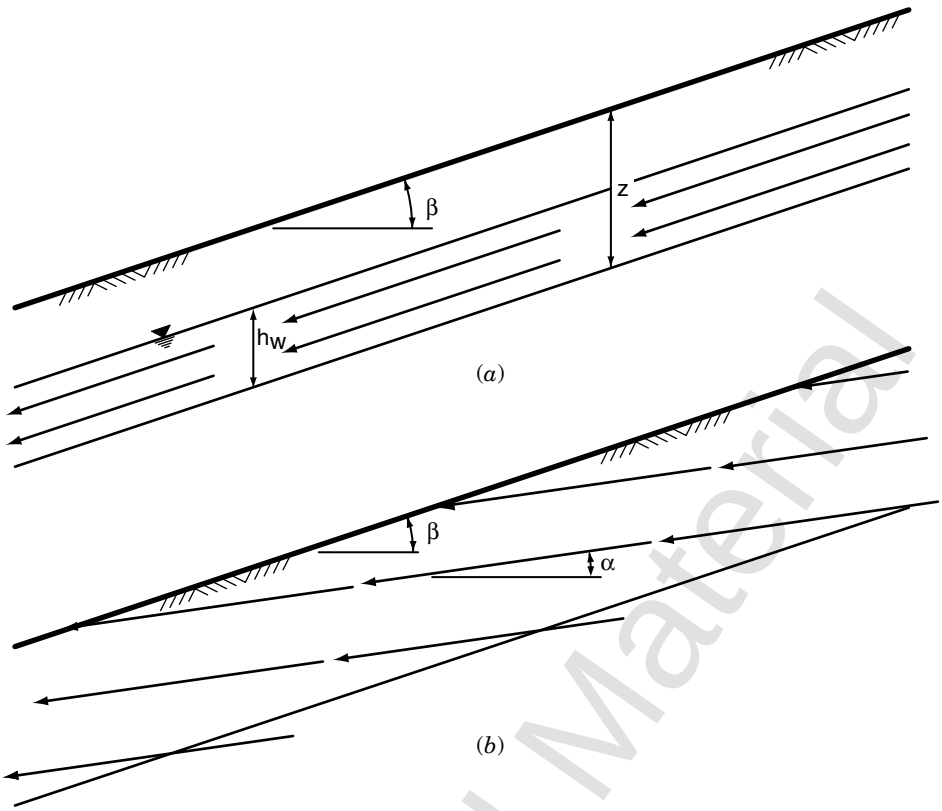


Figure 7.2 Infinite slope with seepage: (*a*) parallel to slope face; (*b*) exiting the slope face.

$$A = 1 - r_u(1 + \tan^2\beta) \tag{7.20}$$

$$B = 1 + \tan^2\beta \tag{7.21}$$

A and B are dimensionless parameters (*stability numbers*) that depend only on the slope angle, and in the case of A, the dimensionless pore water pressure coefficient, r_u. Simple charts for A and B as functions of the slope angle and pore water pressure coefficient, r_u, are presented in the Appendix.

For purely cohesive ($\phi = 0$) soils and homogeneous slopes, the factor of safety can be expressed as

$$F = N_0 \frac{c}{\gamma H} \tag{7.22}$$

where N_0 is a stability number that depends on the slope angle, and in the case of slopes flatter than about 1:1, on the depth of the foundation below the slope. For vertical slopes the value of N_0 according to the Swedish slip circle method is 3.83. This value (3.83) is slightly less than the value of 4 shown in Eq. (7.5) based on a plane slip surface. In general, circular slip surfaces give a lower factor of safety than a plane, especially for flat slopes. Therefore, circles are generally used for analysis of most slopes in cohesive soils. A complete set of charts for cohesive slopes of various inclinations and foundation depths is presented in the Appendix. Procedures are also presented for using average shear strengths with the charts when the shear strength varies.

For slopes with both cohesion and friction, additional dimensionless parameters are introduced. Janbu (1954) showed that the factor of safety could be expressed as

$$F = N_{cf} \frac{c'}{\gamma H} \tag{7.23}$$

where N_{cf} is a dimensionless stability number. The stability number depends on the slope angle, β, the pore water pressures, u, and the dimensionless parameter, $\lambda_{c\phi}$, which is defined as

$$\lambda_{c\phi} = \frac{\gamma H \tan\phi'}{c'} \tag{7.24}$$

Stability charts employing $\lambda_{c\phi}$ and Eq. (7.23) to calculate the factor of safety are presented in the Appen-

Copyrighted Material

Copyright © 2005 John Wiley & Sons Retrieved from: www.knovel.com

dix. These charts can be used for soils with cohesion and friction as well as a variety of pore water pressure and external surcharge conditions.

Although all slope stability charts are based on the assumption of constant shear strength (c, c' and ϕ, ϕ' are constant) or else a simple variation in undrained shear strength (e.g., c varies linearly with depth), the charts can be used for many cases where the shear strength varies. Procedures for using the charts for cases where the shear strength varies are described in the Appendix. Examples for using the charts are also presented in the Appendix.

Recapitulation

- Slope stability charts exist for computing the factor of safety for a variety of slopes and soil conditions.

SPREADSHEET SOFTWARE

Detailed computations for the procedures of slices can be performed in tabular form using a table where each row represents a particular slice and each column represents the variables and terms in the equations presented in Chapter 6. For example, for the case where $\phi = 0$ and the slip surface is a circle, the factor of safety is expressed as

$$F = \frac{\sum c\ \Delta l}{\sum W \sin \alpha} \tag{7.25}$$

A simple table for computing the factor of safety using Eq. (7.25) is shown in Figure 7.3. For the Ordinary Method of Slices with the shear strength expressed in terms of effective stresses, the preferred equation for computing the factor of safety is

$$F = \frac{\sum [c'\ \Delta l + (W \cos \alpha - u\ \Delta l \cos^2\alpha)\tan \phi']}{\sum W \sin \alpha} \tag{7.26}$$

A table for computing the factor of safety using this form of the Ordinary Method of Slices equation is illustrated in Figure 7.4. Tables such as the ones shown in Figures 7.3 and 7.4 are easily represented and implemented in computer spreadsheet software. In fact, more sophisticated tables and spreadsheets can be developed for computing the factor of safety using procedures of slices such as the Simplified Bishop, force equilibrium, and even Chen and Morgenstern's procedures (Low et al., 1998).

The number of different computer spreadsheets that have been developed and used to compute factors of safety is undoubtedly very large. This attests to the usefulness of spreadsheets for slope stability analyses, but at the same time presents several important problems: First, because such a large number of different spreadsheets are used and because each spreadsheet is often used only once or twice, it is difficult to validate spreadsheets for correctness. Also, because one person may write a spreadsheet, use it for some computations and then discard the spreadsheet, results are often poorly archived and difficult for someone else to interpret or to understand later. Electronic copies of the spreadsheet may have been discarded. Even if an electronic copy is maintained, the software that was used to create the spreadsheet may no longer be available or the software may have been updated such that the old spreadsheet cannot be accessed. Hard copies of numerical tabulations from the spreadsheet may have been saved, but unless the underlying equations, formulas, and logic that were used to create the numerical values are also clearly documented, it may be difficult to resolve inconsistencies or check for errors.

Recapitulation

- Spreadsheets provide a useful way of performing calculations by the procedures of slices.
- Spreadsheet calculations can be difficult to check and archive.

COMPUTER PROGRAMS

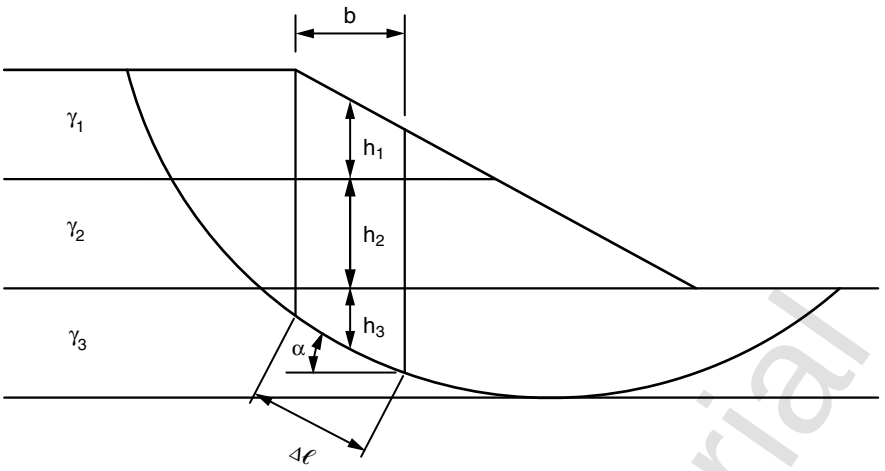
For more sophisticated analyses and complex slope, soil, and loading conditions, computer programs are generally used to perform the computations. Computer programs are available that can handle a wide variety of slope geometries, soil stratigraphies, soil shear strength, pore water pressure conditions, external loads, and internal soil reinforcement. Most programs also have capabilities for automatically searching for the most critical slip surface with the lowest factor of safety and can handle slip surfaces of both circular and noncircular shapes. Most programs also have graphics capabilities for displaying the input data and the results of the slope stability computations.

Types of Computer Programs

Two types of computer programs are available for slope stability analyses: The first type of computer program allows the user to specify as input data the slope geometry, soil properties, pore water pressure condi-

Copyrighted Material

Copyright © 2005 John Wiley & Sons Retrieved from: www.knovel.com



Slice No.	b	h_1	γ_1	h_2	γ_2	h_3	γ_3	$W^{(1)}$	α	$\Delta\ell^{(2)}$	c	$c\Delta\ell$	W sinα
1													
2													
3													
4													
5													
6													
7													
8													
9													
10													
										Summation:			

(1) $W = b \times (h_1\gamma_1 + h_2\gamma_2 + h_3\gamma_3)$
(2) $\Delta\ell = b / \cos\alpha$

$$F = \frac{\Sigma c\Delta\ell}{\Sigma W \sin\alpha}$$

Figure 7.3 Sample table for manual calculations using the Swedish circle ($\phi = 0$) procedure.

tions, external loads, and soil reinforcement, and computes a factor of safety for the prescribed set of conditions. These programs are referred to as *analysis programs*. They represent the more general type of slope stability computer program and are almost always based on one or more of the procedures of slices.

The second type of computer program is the *design program*. These programs are intended to determine what slope conditions are required to provide one or more factors of safety that the user specifies. Many of the computer programs used for reinforced slopes and other types of reinforced soil structures such as soil nailed walls are of this type. These programs allow the user to specify as input data general information about the slope geometry, such as slope height and external loads, along with the soil properties. The programs may also receive input on candidate reinforcement materials such as either the tensile strength of the reinforcement or even a particular manufacturer's product number along with various factors of safety to be achieved. The computer programs then determine what type and extent of reinforcement are required to produce suitable factors of safety. The design programs may be based on either procedures of slices or single-free-body procedures. For example, the logarithmic spiral procedure has been used in several computer

Copyrighted Material

Copyright © 2005 John Wiley & Sons Retrieved from: www.knovel.com

Slice No.	b	h_1	γ_1	h_2	γ_2	h_3	γ_3	W	$\Delta\ell$	α	c'	ϕ'	u	$u\Delta\ell$	W cosα	W cosα - $u\Delta\ell\cos^2\alpha$	(W cosα - $u\Delta\ell\cos^2\alpha$)tanϕ'	c'$\Delta\ell$	W sinα
1																			
2																			
3																			
4																			
5																			
6																			
7																			
8																			
9																			
10																			
															Summation:				

Note: 1. $W = b \times (h_1\gamma_1 + h_2\gamma_2 + h_3\gamma_3)$
2. $\Delta\ell = b / \cos\alpha$

$$F = \frac{\Sigma[(W\cos\alpha - u\Delta\ell\cos^2\alpha)\tan\phi' - c'\Delta\ell]}{\Sigma W\sin\alpha}$$

Figure 7.4 Sample table for manual calculations using the Ordinary Method of Slices and effective stresses.

programs for both geogrid and soil nail design (Leshchinsky, 1997; Byrne, 2003[2]). The logarithmic spiral procedure is very well suited for such applications where only one soil type may be considered in the cross section.

Design programs are especially useful for design of reinforced slopes using a specific type of reinforcement (e.g., geogrids or soil nails) and can eliminate much of the manual trial-and-error effort required. However, the design programs are usually restricted in the range of conditions that can be handled and they often make simplifying assumptions about the potential failure mechanisms. Most analysis program can handle a much wider range of slope and soil conditions.

Automatic Searches for Critical Slip Surface

Almost all computer programs employ one or more schemes for searching for a critical slip surface with the minimum factor of safety. Searches can be performed using both circular and noncircular slip surfaces. Usually, different schemes are used depending on the shape (circular vs. noncircular) of slip surface used. Many different search schemes have been used, and it is beyond the scope of this chapter to discuss these in detail. Nevertheless, several recommendations and guidelines can be offered for searching for a critical slip surface:

1. *Start with circles.* It is almost always preferable to begin searching for a critical slip surface using circles. Very robust schemes exist for searching with circles, and it is possible to examine a large number of possible locations for a slip surface with relatively little effort on the part of the user.
2. *Let stratigraphy guide the search.* For both circular and noncircular slip surfaces, the stratigraphy often suggests where the critical slip surface will be located. In particular, if a relatively weak zone exists, the critical slip surface is likely to pass through it. Similarly, if the weak zone is relatively thin and linear, the slip surface may follow the weak layer and is more likely to be noncircular than circular.
3. *Try multiple starting locations.* Almost all automatic searches begin with a slip surface that the user specifies in some way. Multiple starting locations should be tried to determine if one location leads to a lower factor of safety than another.

[2] Byrne has utilized the log spiral procedure in an unreleased version of the GoldNail software. One of the authors (Wright) has also used the log spiral successfully for this purpose in unreleased software for analyzing soil nail walls.

Copyrighted Material

Copyright © 2005 John Wiley & Sons Retrieved from: www.knovel.com

4. *Be aware of multiple minima*. Many search schemes are essentially optimization schemes that seek to find a single slip surface with the lowest factor of safety. However, there may be more than one ''local'' minimum and the search scheme may not necessarily find the local minimum that produces the lowest factor of safety overall. This is one of the reasons why it is important to use multiple starting locations for the search.
5. *Vary the search constraints and other parameters*. Most search schemes require one or more parameters that control how the search is performed. For example, some of the parameters that may be specified include:
   - The incremental distances that the slip surface is moved during the search
   - The maximum depth for the slip surface
   - The maximum lateral extent of the slip surface or search
   - The minimum depth or weight of soil mass above the slip surface
   - The maximum steepness of the slip surface where it exits the slope
   - The lowest coordinate allowed for the center of a circle (e.g., to prevent inversion of the circle)

   Input data should be varied to determine how these parameters affect the outcome of the search and the minimum factor of safety.

A relatively large number of examples and benchmarks can be found in the literature for the factor of safety for a particular slip surface. However, many fewer examples can be found to confirm the location of the most critical slip surface (lowest factor of safety), even though this may be the more important aspect of verification. For complex slopes, much more effort is usually spent in a slope stability analysis to verify that the most critical slip surface is found than is spent to verify that the factor of safety for a given slip surface has been computed correctly.

Restricting the Critical Slip Surfaces of Interest

In general, all areas of a slope should be searched to find the critical slip surface with the minimum factor of safety. However, is some cases it may be desirable to search only a certain area of the slope by restricting the location of trial slip surfaces. There are two common cases where this is appropriate. One case is where there are insignificant modes of failure that lead to low factors of safety, but the consequences of failure are small. The other case is where the slope geometry is such that a circle with a given center point and radius does not define a unique slip surface and slide mass. These two cases are described and discussed further below.

Insignificant modes of failure. For cohesionless slopes it has been shown that the critical slip surface is a very shallow plane, essentially coincident with the face of the slope. However, the consequences of a slide where only a thin layer of soil is involved may be very low and of little significance. This is particularly the case for some mine tailings disposal dams. In such cases it is desirable to investigate only slip surfaces that have some minimum size and extent. This can be done in several ways, depending on the particular computer program being used:

- The slip surfaces investigated can be required to have a minimum depth.
- The slip surfaces investigated can be forced to pass through a specific point at some depth below the surface of the slope.
- The soil mass above the slip surface can be required to have a minimum weight.
- An artificially high shear strength, typically expressed by a high value of cohesion, can be assigned to a zone of soil near the face of the slope so that shallow slip surfaces are prevented. In doing so, care must be exercised to ensure that slip surfaces are not unduly restricted from exiting in the toe area of the slope.

Ambiguities in slip surface location. In some cases it is possible to have a circle where more than one segment of the circle intersects the slope (Figure 7.5). In such cases there is not just a single soil mass above the slip surface, but rather there are multiple, disassociated soil masses, probably with different factors of safety. To avoid ambiguities in this case, it is necessary to be able to designate that only a particular portion of the slope is to be analyzed.

Recapitulation

- Computer programs can be categorized as design programs and analysis programs. Design programs are useful for design of simple reinforced slopes, while analysis programs generally can handle a much wider range of slope and soil conditions.
- Searches to locate a critical slip surface with a minimum factor of safety should begin with circles.

Copyrighted Material

Copyright © 2005 John Wiley & Sons Retrieved from: www.knovel.com

- Multiple searches with different starting points and different values for the other parameters that affect the search should be performed to ensure that the most critical slip surface is found.
- In some case it is appropriate to restrict the region where a search is conducted; however, care must be taken to ensure that an important slip surface is not overlooked.

VERIFICATION OF ANALYSES

Most slope stability analyses are performed using general-purpose computer programs. The computer programs offer a number of features and may involve tens of thousands, and sometimes millions, of lines of computer code with many possible paths through the logic, depending on the problem being solved. Forester and Morrison (1994) point out the difficulty of checking even simple computer programs with multiple combinations of paths through the software. Consider, for example, a comprehensive computer program for slope stability analysis that contains the features listed in Table 7.1. Most of the more sophisticated computer programs probably contain at least the number of options or features listed in this table. Although some programs will not contain all of the options listed, they may contain others. A total of 40 different features and options is listed in Table 7.1. If we consider just two different possibilities for the input values for each option or feature, there will be a total of over 1×10^{12} ($= 2^{40}$) possible combinations and paths through the software. If we could create, run, and verify problems to test each possible combination at the rate of one test problem every 10 minutes, over 20 million years would be required to test all possible combinations, working 24 hours a day, 7 days a week. Clearly, it is not possible to test sophisticated computer programs for all possible combinations of data, or even a reasonably small fraction, say 1 of 1000, of the possible combinations. Consequently, there is a significant possibility that any computer program being used has not been tested for the precise combination of paths involved in a particular problem.

Because it is very possible that any computer program has not been verified for the particular combination of conditions the program is being used for, some form of independent check should be made of the results. This is also true for other methods of calculation. For example, spreadsheets are just another form of computer program, and the difficulty of verifying spreadsheet programs was discussed earlier. It is also possible to make errors in using slope stability charts and even in using simple equations. Furthermore, the simple equations generally are based on approximations that can lead to important errors for some applications. Consequently, regardless of how slope stability computations are performed, some independent check should be made of the results. A number of examples of slope stability analyses and checks that can be made are presented in the next section.

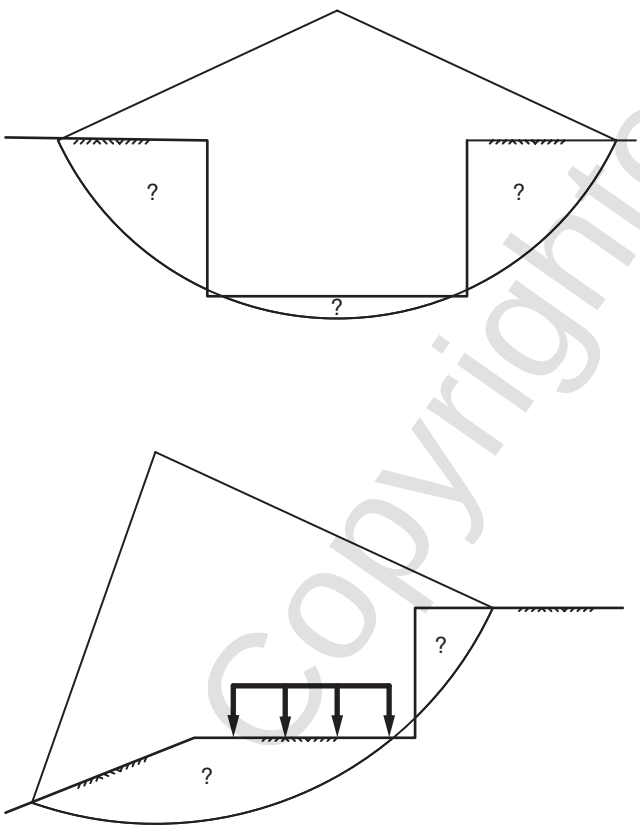


Figure 7.5 Cases where the slide mass defined by a circular slip surface is ambiguous and may require selective restriction.

Recapitulation

- Because of the large number of possible paths through most computer programs, it is likely most programs have not been tested for the precise combination of paths involved in any particular analysis.
- Some check should be made of the results of slope stability calculations, regardless of how the calculations are performed.

Copyrighted Material

Copyright © 2005 John Wiley & Sons Retrieved from: www.knovel.com

Table 7.1 Possible Options and Features for a Comprehensive Slope Stability Computer Program

	Soil profile lines—stratigraphy
Soil shear strength	c–ϕ soil—total stresses
	c'–σ' soil—effective stresses
	Curved Mohr failure envelope—total stresses
	Curved Mohr failure envelope—effective stresses
	Undrained shear strength varies with depth below horizontal datum
	Undrained shear strength defined by contour lines or interpolation
	Shear strength defined by a c/p ratio
	Anisotropic strength variation—undrained strength and total stresses
	Anisotropic strength variation—drained strength and effective stresses
	Consolidated–undrained shear strength (e.g., for rapid drawdown—linear strength envelopes)
	Consolidated–undrained shear strength (e.g., for rapid drawdown—curved strength envelopes)
	Structural materials (e.g., steel, concrete, timber)
Pore water pressure	Constant pore water pressure
	Constant pore pressure coefficient, r_u
	Piezometric line
	Phreatic surface
	Interpolated values of pore water pressure (e.g., from finite element analyses)
	Interpolated values of pore water pressure coefficient, r_u
	Slope geometry
	Left vs. right face of slope analyzed
	Distributed surface loads (e.g., water)
	Line loads
Reinforcement	Geotextiles
	Geogrids
	Soil nails
	Tieback anchors
	Piles
	Piers
Slip surface(s)	Individual circle
	Individual noncircular slip surface
	Systematic search with circles
	Random search with circles
	Systematic search with noncircular slip surfaces
	Random search with noncircular slip surfaces
Procedure of analysis	Simplified Bishop procedure
	Spencer's procedure
	Corps of Engineers' Modified Swedish procedure
	Simplified Janbu procedure
	Chen and Morgenstern's procedure

EXAMPLES FOR VERIFICATION OF STABILITY COMPUTATIONS

Ten example slopes were selected for the slope stability analyses presented in this section. These examples were selected with two purposes in mind: First, to illustrate the different methods for computing the factor of safety that were discussed in the preceding sections of this chapter, and second, to illustrate several important details and features of slope stability analyses. For example, one problem addresses the use of submerged unit weights. Several other problems illustrate the differences among various procedures of slices. Some of these and other examples illustrate the importance of locating the critical slip surface. Most of the examples are presented with enough detail that they can be used as benchmarks for verifying results of calculations using other means (e.g., with other computer programs).

Copyrighted Material

Copyright © 2005 John Wiley & Sons Retrieved from: www.knovel.com

The 10 example problems selected for analysis are summarized in Table 7.2. Each example is described briefly and the methods of calculation (simple equations, charts, spreadsheets, and computer programs) are indicated. Any calculations presented using computer programs were performed with the UTEXAS4 software (Wright, 1999) unless otherwise stated. The summary also indicates whether analyses were performed for short- or long-term stability conditions. Additional features illustrated by each example are indicated in the last column of Table 7.2. The 10 cases listed in this table provide a useful collection of problems for computer program verification.

Example 1: Unbraced Vertical Cut in Clay

Tschebotarioff (1973) describes the failure of a vertical excavated slope that was made for a two-story basement in varved clay. The excavation was made, without bracing, to a depth of 22 ft on one side and 31.5 ft on the other side. The average unconfined compressive strength of the clay from an investigation nearby was reported to be 1.05 tons/ft^2 and the unit weight of the clay was 120 lb/ft^3. Factors of safety were calculated for the deeper of the two cuts (Figure 7.6) using the equation for a vertical slope with a plane slip surface, and using the slope stability charts presented in the Appendix. Calculations were also performed using a computer program. For an undrained shear strength, S_u of 1050 psf ($= q_u/2$), the factor of safety for a plane slip surface is calculated as

$$F = \frac{4c}{\gamma H} = \frac{(4)(1050)}{(120)(31.5)} = 1.11 \qquad (7.27)$$

Using Janbu's charts for $\phi = 0$ presented in the Appendix, the factor of safety is calculated as

$$F = N_0 \frac{c}{\gamma H} = (3.83) \frac{1050}{(120)(31.5)} = 1.06 \qquad (7.28)$$

Calculations with circles using the computer program resulted in a factor of safety of 1.06. The calculations with the charts confirm the results with the computer program, and both show that circular slip surfaces give a slightly lower factor of safety than plane slip surfaces.

Although the foregoing calculations are in close agreement, they may not correctly reflect the true factor of safety of the slope. Terzaghi (1943) pointed out that the upper part of the soil adjacent to a vertical slope is in tension. If the soil cannot withstand tension, cracks will form and the factor of safety will be reduced. Terzaghi showed that if one conservatively estimates that a crack will form to a depth equal to one-half the slope height, the equation for the factor of safety (assuming a planar slip surface) becomes

$$F = 2.67 \frac{c}{\gamma H} \qquad (7.29)$$

Thus, for the slope described above,

$$F = \frac{(2.67)(1050)}{(120)(31.5)} = 0.74 \qquad (7.30)$$

which would clearly indicate that the slope was not stable. A computed factor of safety less than 1.0 for this case seems reasonable, because the slope failed and the unconfined compression tests that were used to measure the shear strength would be expected to underestimate strength due to sample disturbance.

In the first calculations with the computer program, tension was observed on the bottoms of several of the slices near the upper part of the slope. Subsequently, a series of slope stability calculations was performed in which vertical tension cracks were introduced, beginning with a crack depth of 1 ft, and successively increasing the crack depth in 1-ft increments until there was no longer tension. The assumed crack depths, corresponding factors of safety, and minimum normal stresses on the base of slices are summarized in Table 7.3. If we take the factor of safety as being the value where the tensile stresses are first eliminated, we would conclude that the factor of safety is less than 1 (between 0.96 and 0.99).

For this example the stability calculations support the behavior observed quite well. However, the closeness of the factor of safety to unity may be due in part to compensating errors caused by factors that were not considered. The shear strengths used were based on unconfined compression tests, which typically underestimate the shear strength. Thus, it is likely that the undrained shear strength of the clay was actually greater than what was assumed. At the same time, because the slope was excavated, the unloading due to excavation would cause the soil to swell gradually and lose strength with time. Also, it is possible that vertical cracks may have opened to substantial depths. It is possible to imagine that the undrained strength measured in more appropriate UU tests would have been considerably higher than the shear strength used, while losses of strength due to swell and the development of deep tension cracks could have reduced the stability by a substantial amount. These offsetting factors could have affected the stability of the slope significantly, and it can be seen that the failure may have taken place

Copyrighted Material

Copyright © 2005 John Wiley & Sons Retrieved from: www.knovel.com

Table 7.2 Summary of Example Problems for Verification of Slope Stability Analyses

			Methods of analysis and verification of results												
			Simple equations			Charts			Spreadsheets				Computer program		
No.	Description	Short or long term	Vertical slope—plane	Bearing capacity	Infinite slope	$\phi = 0$: Janbu	$\phi = 0$: Hunter and Schuster	c, ϕ Soil: Janbu	$\phi = 0$	OMS	Simplified Bishop	Force equilibrium	UTEXAS4	Other	Additional features
1	Unbraced vertical cut in saturated clay (after Tschebotarioff); including effects of tension crack	S	Y			Y							Y		Effects of tension and a tension crack.
2	LASH terminal: submerged slope excavated in saturated, nearly normally consolidated clay	S					Y						Y		Use of total unit weights and pore water pressures vs. submerged unit weights.
3	Bradwell slip—excavated slope in stiff-fissured clay	S							Y				Y		Application of Janbu correction factor in simplified Janbu procedure. Slope may fail even with high factor of safety.
4	Hypothetical example of cohesionless slope ($c = 0$) on saturated clay ($\phi = 0$) foundation	S		Y						Y			Y		Application of Janbu correction factor in simplified Janbu procedure. Relatively large differences in F by various procedures.
5	Oroville Dam—high rockfill dam	L			Y								Y		Stability computations with a curved Mohr shear strength envelope.

Copyrighted Material

Copyright © 2005 John Wiley & Sons Retrieved from: www.knovel.com

6	James Bay dike—embankments constructed on soft clay foundation	S				Y	Y		Importance of finding critical slip surface.
7	Homogeneous earth dam with steady-state seepage	L		Y			Y		Effects of how pore water pressures are represented (by flow net, piezometric line, phreatic surface). Illustrates effects of pore pressure in Ordinary Method of Slices.
8	Zoned (or clay core) earth dam with steady-state seepage	L			Y		Y		Effects of how pore water pressures are represented (by flow net, piezometric line, phreatic surface).
9	Reinforced slope (1): embankment on a soft clay foundation	S					Y	Y	Reinforced slope analysis; influence of location of critical circle.
10	STABGM reinforced slope (2): steep reinforced slope	L					Y	Y	Reinforced slope analysis; influence of location of critical circle.

Copyrighted Material

Copyright © 2005 John Wiley & Sons Retrieved from: www.knovel.com

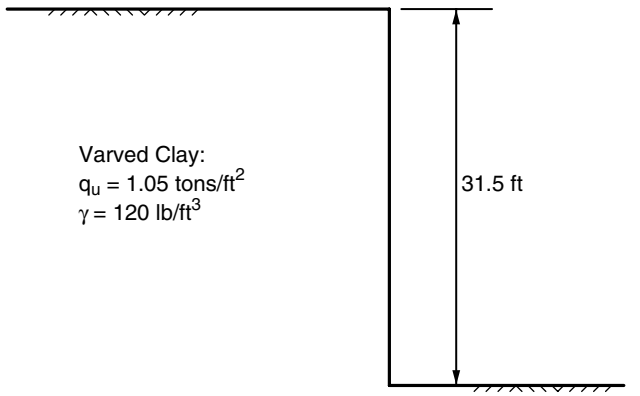


Figure 7.6 Unbraced vertical cut in clay described by Tschebotarioff (1973).

Table 7.3 Variation in the Factor of Safety and Minimum Normal Stress on the Slip Surface with the Assumed Depth of Tension Crack

Assumed crack depth (ft)	Minimum normal stress on slip surface (base of slices) (psf)	Calculated factor of safety
0	−241	1.06
1	−160	1.04
2	−67	1.01
3	−62	0.99
4	40	0.96

under conditions quite different from what was assumed in the stability calculations.

Recapitulation

- Slope stability charts, the computer program, and the simple equation for stability of a vertical cut based on plane slip surfaces all gave nearly identical values for the factor of safety.
- Plane slip surfaces, compared to circles, give similar but slightly higher values for the factor of safety of a vertical slope.
- Tensile stresses may develop behind the crest of steep slopes in clay and may lead to cracking that will substantially reduce the stability of the slope.
- Close agreement between computed and actual factors of safety may be fortuitous and a result of multiple large errors that compensate.

Example 2: Underwater Slope in Soft Clay

Duncan and Buchignani (1973) described the failure of a slope excavated underwater in San Francisco Bay. The slope was part of a temporary excavation and was designed with an unusually low factor of safety to minimize construction costs. During construction a portion of the excavated slope failed. A drawing of the slope cross section is shown in Figure 7.7. The undrained shear strength profile is presented in Figure 7.8. The original design factor of safety based on undrained shear strengths was reported by Duncan and Buchignani to be 1.17.

Recently (2003), new slope stability calculations were performed by the writers, first using a computer program with Spencer's procedure of slices. The minimum factor of safety calculated was 1.17. Because the undrained shear strength for the clay in the slope increases linearly with depth, Hunter and Schuster's (1968) slope stability charts described in the Appendix can also be used to compute the factor of safety. The factor of safety computed using these charts is 1.18.

The slope stability calculations described above were performed using submerged (buoyant) unit weights to account for the slope being fully submerged. Submerged unit weights are convenient to use when the computations are being performed with either slope stability charts or by hand using a spreadsheet. Submerged unit weights can be used for this example because there was no seepage force (no flow of water). However, in general when using computer programs it is preferable to use total unit weights and to specify external and internal water pressures. Computer calculations were repeated for this slope using total unit weights and distributed loads on the surface of the slope to represent the water pressures. The factor of safety was again found to be 1.17. This not only confirms what is expected but provides a useful check on the calculations of the weights of slices and the forces due to external distributed loads calculated by the computer program.

A simple and useful check of any computer program is to perform separate sets of slope stability calculations for a submerged slope (with no flow) using (1) submerged unit weights and (2) total unit weights with water pressures. If the computer program is working properly and being used properly, it should give the same result for both sets of calculations.[3]

[3]This may not be true with force equilibrium procedures with inclined interslice forces. Similar results may not be obtained with submerged unit weights and total unit weights plus water pressures when the interslice forces are total forces, due to both earth and water pressures, as described in Chapter 6. In this case the differences in factors of safety calculated using submerged unit weights and total unit weights plus water pressures may be large.

Copyrighted Material

Copyright © 2005 John Wiley & Sons Retrieved from: www.knovel.com

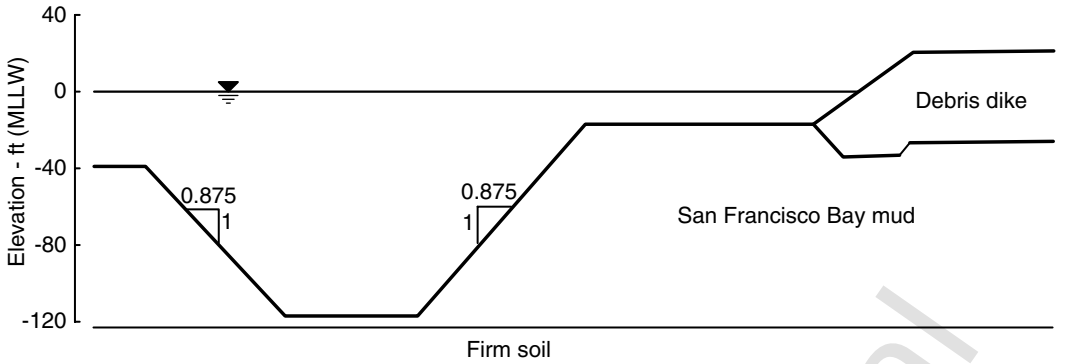


Figure 7.7 Underwater slope in San Francisco Bay mud described by Duncan and Buchignani (1973) and Duncan (2000).

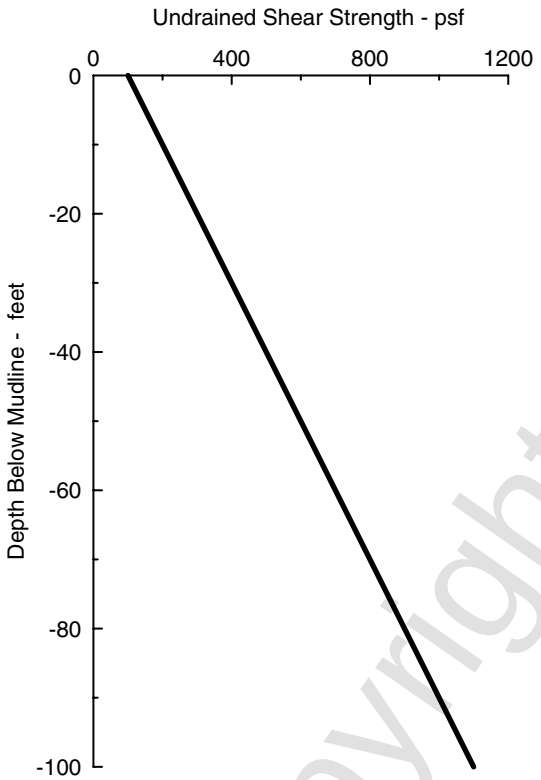


Figure 7.8 Undrained shear strength profile for underwater slope in San Francisco Bay mud. (From Duncan, 2000.)

Although the calculations presented above confirm the factor of safety calculated by Duncan and Buchignani (1973) and indicate that the slope would be expected to be stable, a portion of the slope failed, as noted earlier. Duncan and Buchignani (1973) showed that the effects of sustained loading (creep) under undrained conditions was probably sufficient to reduce the shear strength and cause the failure. More recent reliability analyses by Duncan (2000) have shown that the probability of failure was almost 20%. This probability of failure is consistent with the fact that about 20% of the length of the slope actually failed. Given the accuracy with which such analyses can be made, the close agreement between the probability of failure and the fraction of the slope that failed is probably fortuitous.

Because this slope was only temporary, it was appropriate to compute the stability using undrained shear strengths. However, if the slope was permanent, much lower drained shear strengths would apply. As the soil swells due to unloading by excavation, the shear strength would gradually be reduced. Eventually, the fully drained shear strength would become applicable. Representative values of the drained (effective stress) shear strength parameters for San Francisco Bay mud are $c' = 0$, $\phi' = 34.5°$ (Duncan and Seed, 1966*b*). For a fully submerged slope and $c' = 0$, the factor of safety can be calculated using the equation for an infinite slope as

$$F = \frac{\tan \phi'}{\tan \beta} = \frac{\tan 34.5°}{1/0.875} = 0.60 \qquad (7.31)$$

Clearly, this factor of safety (0.60) is much less that the factor of safety (1.17) based on undrained shear strengths, indicating that a substantial reduction in factor of safety would have occurred if the excavated trench had not been filled with sand.

Recapitulation

- Identical values for the factor of safety were obtained using a computer program and a slope stability chart.
- Either submerged unit weights or total unit weights and water pressures may be used to compute the stability of a submerged slope when there is no flow.

Copyrighted Material

Copyright © 2005 John Wiley & Sons Retrieved from: www.knovel.com

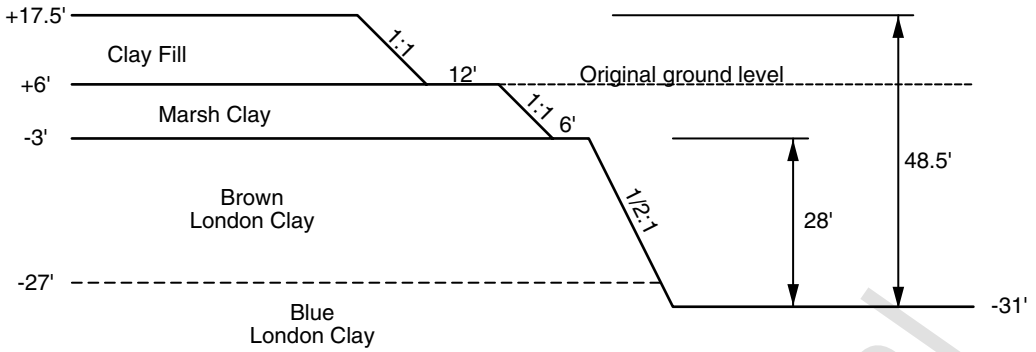


Figure 7.9 Cross section of excavated slope for reactor 1 at Bradwell. (From Skempton and LaRochelle, 1965.)

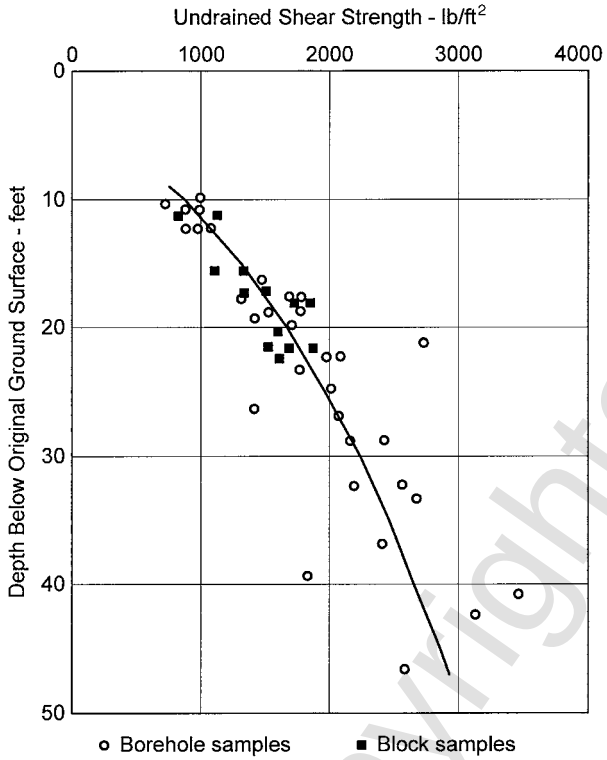


Figure 7.10 Undrained shear strength profile for reactor 1 excavation slope at Bradwell. (From Skempton and LaRochelle, 1965.)

- Even though the calculated factor of safety was greater than unity (1.17), the slope failed due to creep strength loss.
- For an excavated slope, the short-term factor of safety based on undrained conditions may be much higher than the long-term factor of safety based on drained conditions.

Example 3: Excavated Slope in Stiff-Fissured Clay

Skempton and LaRochelle (1965) describe a deep excavation in the London Clay at Bradwell. A cross section of the excavation for reactor 1 is shown in Figure 7.9. The excavation is 48.5 ft deep. The lower 28 ft of the excavation is in London Clay and is inclined at $\frac{1}{2}$(horizontal):1(vertical). The London Clay is overlain by 9 ft of Marsh clay where the excavation slope was inclined at 1:1 (45°). Approximately 11.5 ft of clay from the excavation was placed at the top of the excavation, over the marsh clay. The clay fill was also inclined at 1:1.

Short-term stability analyses were performed for the slope using undrained shear strengths. The marsh clay was reported to have an average undrained shear strength of 300 psf and a total unit weight of 105 pcf. The clay fill was assumed to crack to the full depth of the fill (11.5 ft), and thus its strength was ignored. Skempton and LaRochelle reported a total unit weight of 110 pcf for the fill. The undrained shear strength profile for the London Clay is shown in Figure 7.10. The undrained shear strength increases at a decreasing

Table 7.4 Summary of Short-Term Slope Stability Analyses for an Excavated Slope in Stiff-Fissured Clay: The Bradwell Slip

Procedure of slices	Factor of safety
Spencer	1.76
Simplified Bishop	1.76
Corps of Engineers' Modified Swedish	1.80
Simplified Janbu—no correction	1.63
Simplified Janbu—with correction, f_0	1.74

Copyrighted Material

Copyright © 2005 John Wiley & Sons Retrieved from: www.knovel.com

rate with depth. A representative unit weight for the London Clay at the site is 120 pcf.

Stability computations were first performed for this example using a computer program and several procedures of slices. The resulting factors of safety are summarized in Table 7.4. The values for the factor of safety are as expected: Spencer's procedure and the Simplified Bishop procedure give identical values because they both satisfy moment equilibrium; there is only one value for the factor of safety that will satisfy moment equilibrium for a circular slip surface. The Corps of Engineers' Modified Swedish procedure, a force equilibrium procedure, overestimates the factor of safety compared to procedures that satisfy complete equilibrium, as is commonly the case. The Simplified Janbu procedure (force equilibrium with horizontal interslice forces) without Janbu et al.'s (1956) correction factor underestimates the factor of safety, as is also typically the case. The correction factor, f_0, for the Simplified Janbu procedure was calculated from the following equation presented by Abramson et al., (2002):

$$f_0 = 1 + b_1 \left[\frac{d}{L} - 1.4\left(\frac{d}{L}\right)^2 \right] \qquad (7.32)$$

where b_1 is a factor that depends on the soil type (c and ϕ) and d/L represents the slide depth-to-length ratio. For $\phi = 0$, b_1 is 0.69 and the depth-to-length ratio for the critical circle found for the Simplified Janbu procedure is 0.13. The resulting correction factor calculated from Eq. (7.32) is 1.07 and the corrected factor of safety is 1.74 (= 1.07 × 1.63). This corrected value (1.74) for the factor of safety by the Simplified Janbu procedure agrees well with the value (1.76) calculated by procedures that satisfy moment equilibrium.

The factor of safety was also calculated manually using a spreadsheet program based on the Ordinary Method of Slices. Because ϕ is zero for this problem and the Ordinary Method of Slices satisfies moment equilibrium, the Ordinary Method of Slices should give the same value for the factor of safety as Spencer's and the Simplified Bishop procedures. There is no need to use a more complex procedure than the Ordinary Method of Slices for this case. The calculations for the Ordinary Method of Slices are shown in Figure 7.11. As expected, the factor of safety is 1.76, which is the same as the value shown previously for Spencer's and the Simplified Bishop procedures.

Although the factor of safety calculated for this slope is almost 1.8, the slope failed approximately 5 days after excavation was completed. Skempton and LaRochelle (1965) discuss the probable causes of failure. These include overestimates of the shear strength due to testing of samples of small size, strength losses due to sustained loading (creep), and the presence of fissures. Skempton and LaRochelle concluded that the

Slice No.	b (ft)	h_{fill} (ft)	γ_{fill} (pcf)	h_{marsh} (ft)	γ_{marsh} (pcf)	h_{clay} (ft)	γ_{clay} (pcf)	W (pounds)	α (deg)	$\Delta\ell$ (ft)	c (psf)	$c\Delta\ell$	W sinα
1	10.8	11.5	110	4.5	105	-	-	18,748	39.8	14.1	300	4,215	12,008
2	9.1	11.5	110	9.0	105	3.2	120	23,637	35.1	11.1	1069	11,908	13,602
3	11.5	5.8	110	9.0	105	9.8	120	31,665	30.5	13.3	1585	21,157	16,082
4	12.0	-	-	9.0	105	16.1	120	34,466	25.6	13.3	1968	26,183	14,873
5	9.0	-	-	4.5	105	20.7	120	26,857	21.3	9.7	2222	21,461	9,636
6	6.0	-	-	-	-	23.4	120	16,862	18.3	6.3	2349	14,841	5,284
7	5.5	-	-	-	-	19.7	120	13,002	16.0	5.7	2429	13,900	3,590
8	8.5	-	-	-	-	7.5	120	7,645	13.3	8.7	2503	21,861	1,759
										Summations:		135,525	76,835

$$F = \frac{135{,}525}{76{,}835} = 1.76$$

Figure 7.11 Manual calculations by the Ordinary Method of Slices for short-term stability of the slope at Bradwell.

Copyrighted Material

Copyright © 2005 John Wiley & Sons Retrieved from: www.knovel.com

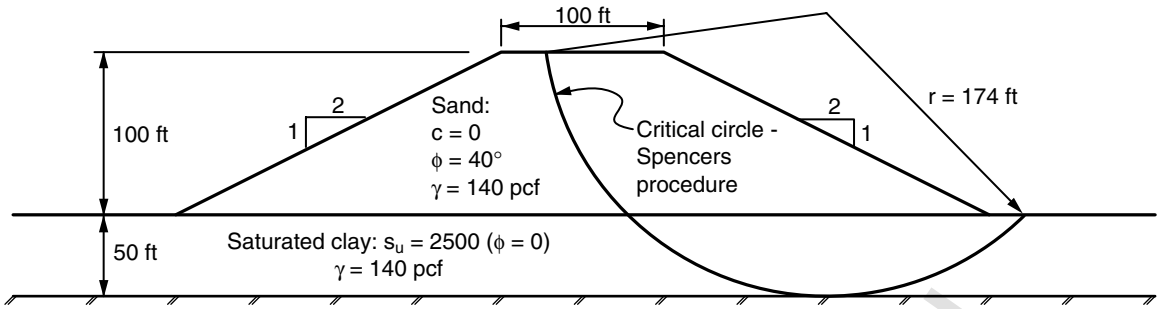


Figure 7.12 Cohesionless fill slope on saturated clay foundation.

opening of fissures and a lower, residual strength along the fissures were probable causes of failure of the slope, even though the factor of safety computed based on undrained shear strengths was relatively high.

Recapitulation

- Spencer's, the Simplified Bishop, and Ordinary Method of Slices procedures all gave the same value for the factor of safety for circular slip surfaces because $\phi = 0$, and all these procedures satisfy moment equilibrium.
- The computer solution and the manual solution using a spreadsheet gave the same value for the factor of safety.
- The Corps of Engineers' Modified Swedish procedure overestimated the factor of safety for this case by a small amount (2%).
- The Simplified Janbu procedure without the correction factor applied underestimated the factor of safety by about 7%.
- The corrected factor of safety by the Simplified Janbu procedure agrees within 1% with the value of the factor of safety calculated using methods that satisfy moment equilibrium.
- Although the factor of safety for short-term stability was much greater than 1, the slope failed approximately five days after construction, due to several factors that influenced the shear strength.

Example 4: Cohesionless Slope on Saturated Clay Foundation

The fourth example is for a hypothetical embankment constructed of cohesionless granular material resting on a saturated clay ($\phi = 0$) foundation, as shown in Figure 7.12. The embankment is assumed to drain almost instantaneously, and thus its strength will not change over time. The clay in the foundation is expected to consolidate with time and its strength is expected to increase with time. Therefore, the critical period (lowest factor of safety) for the embankment should be immediately after construction.

Soil shear strength and unit weight properties are shown in Figure 7.12. Drained (effective stress) shear strength parameters are shown for the embankment, and undrained shear strengths are shown for the clay foundation. Stability computations were first performed using a computer program and several procedures of slices. The minimum factors of safety for various procedures are summarized in Table 7.5, and the critical slip surface by Spencer's procedure is shown in Figure 7.12.

As expected, the Simplified Bishop procedure gives a value for the factor of safety that is very close to the one calculated by Spencer's procedure. The Simplified Janbu procedure without the correction factor applied gives a factor of safety that is approximately 10% lower, but the corrected value (1.16) agrees closely with the values by the Simplified Bishop and Spencer's procedures. The Corps of Engineers' Modified Swedish procedure produced a factor of safety about 25% higher than the value by Spencer's procedure. The much higher value clearly demonstrates the potentially

Table 7.5 Summary of Slope Stability Analyses for a Cohesionless Embankment Supported by a Saturated Clay Foundation

Procedure of slices	Factor of safety
Spencer	1.19
Simplified Bishop	1.22
Corps of Engineers' Modified Swedish	1.54
Simplified Janbu—no correction	1.07
Simplified Janbu—with correction f_0[a]	1.16

[a]Correction based on Eq. (7.32) with $b_1 = 0.5$ and $d/L = 0.34$; $f_0 = 1.09$.

Copyrighted Material

Copyright © 2005 John Wiley & Sons Retrieved from: www.knovel.com

unconservative nature of the Modified Swedish force equilibrium procedure.

The factor of safety was also computed using the Ordinary Method of Slices with a spreadsheet program for the critical circle found by Spencer's procedure. The computations are shown in Figure 7.13. The computed factor of safety is 1.08, approximately 10% less than the value calculated using Spencer's procedure. Differences of this order (10%) are typical for cases like this one where c and ϕ vary significantly along the slip surface.

As an additional, approximate check on the stability of the embankment, the bearing capacity equation [Eq. (7.10)] was used to calculate a factor of safety. This gave

$$F = 5.53 \frac{2500}{(140)(100)} = 0.99 \qquad (7.33)$$

Although the bearing capacity solution represented by Eq. (7.33) underestimates the stability of the embankment in this example, it provides a simple and convenient way of preliminary screening for potential problems. In general, if the factor of safety for bearing capacity is near or below 1, the factor of safety is likely to be marginal and additional, more detailed analyses are probably warranted.

Recapitulation

- Spencer's procedure and the Simplified Bishop procedure give very similar values for the factor of safety.
- The Corps of Engineers' Modified Swedish procedure can substantially overestimate the factor of safety.
- The Simplified Janbu procedure without the correction factor applied underestimated the factor of safety, but the value is improved by applying the correction.
- The Ordinary Method of Slices underestimates the factor of safety but provides a convenient way of checking a computer solution using more accurate methods.
- The simple equation for bearing capacity on a saturated clay foundation gives a conservative estimate of stability but provides a useful tool for screening for stability problems.

Example 5: Cohesionless Embankment (Oroville Dam)—Curved Mohr–Coulomb Envelope

The next example is of the Oroville Dam, in particular, the stability of the downstream slope (Figure 7.14). The downstream slope is composed of rockfill (amphibolite gravel). As for most granular materials, the Mohr failure envelope is curved. Due to the great height of the Oroville Dam (778 ft) and the large variation in the pressures from the top to the bottom of the embankment, the curved Mohr failure envelope requires special consideration for the slope stability computations.

Curved (nonlinear) Mohr failure envelope. For this example the shear strength of the downstream shell material is characterized by a *secant friction angle* (i.e., $\tan \phi' = \tau_f / \sigma'_f$), which represents the slope of a line drawn from the origin of the Mohr diagram to a point on the Mohr failure envelope. As discussed in Chapter 5, the secant friction angle varies with confining pressure and can be related to the minor principal stress, σ'_3 by

$$\phi' = \phi_0 - \Delta\phi \log_{10} \frac{\sigma'_3}{p_a} \qquad (7.34)$$

where ϕ_0 is the friction angle for a confining pressure (σ'_3) of 1 atm, $\Delta\phi$ is the change in friction angle per log-cycle (10-fold) change in confining pressure, and p_a is atmospheric pressure. Duncan et al. (1989) summarize shear strength data for the Oroville dam and report values of $\phi_0 = 51°$ and $\Delta\phi = 6°$ for the shell material.

For slope stability computations the shear strength needs to be defined by a Mohr failure envelope that expresses the shear strength, τ, as a function of the normal stress, σ or σ', depending on whether total or effective stress analyses are being performed. The normal stress, σ', should be the normal stress on the failure plane at failure, σ'_{ff}. The relationship between σ'_{ff} and confining pressure, σ'_3, depends on the shear strength parameters. For a cohesionless soil ($c' = 0$) the relationship is expressed as

$$\sigma'_{ff} = \sigma'_{3f} \frac{\cos^2 \phi'}{1 - \sin \phi'} \qquad (7.35)$$

Ratios of σ'_{ff} to σ'_{3f} are tabulated in Table 7.6 for a range in friction angles that are representative for granular materials. The ratios shown in Table 7.6 vary with friction angle; however, it is convenient to assume that the ratio, $\sigma'_{ff}//\sigma'_{3f}$ is constant and equal to 1.5 for any value of ϕ'. This assumption has very little effect on the Mohr failure envelope that is subsequently computed. To illustrate this, consider a material with a value of ϕ_0 of 40° and $\Delta\phi$ of 10°. Computation of the friction angles, ϕ', for values of effective normal stress, σ' (= σ'_{ff}), of 100, 1000, and 10,000 psf are shown in Table 7.7. For each value of the effective

Copyrighted Material

Copyright © 2005 John Wiley & Sons Retrieved from: www.knovel.com

Slice No.	b (ft)	h_{fill} (ft)	γ_{fill} (pcf)	h_{clay} (ft)	γ_{clay} (pcf)	W (lb)	$\Delta\ell$	α	c (psf)	ϕ (deg)	W cosα	(W cosα) tanϕ'	c'$\Delta\ell$	W sinα
1	10.7	19.2	140	0.0	125	28706	40	74.5	0	40	7666	6432	0	27664
2	19.0	56.0	140	0.0	125	148726	40	61.6	0	40	70653	59285	0	130872
3	22.5	86.8	140	0.0	125	273040	35	49.6	0	40	176932	148464	0	207956
4	22.7	100.0	140	9.3	125	343995	29	39.3	2500	0	266206	0	73301	217869
5	35.2	91.2	140	28.0	125	572546	40	28.1	2500	0	504909	0	99788	269954
6	38.5	72.8	140	42.6	125	597628	40	15.3	2500	0	576542	0	99796	157348
7	27.3	56.3	140	49.0	125	382166	27	4.4	2500	0	381040	0	68427	29322
8	39.7	39.6	140	47.8	125	456562	40	-6.4	2500	0	453677	0	99781	-51247
9	37.7	20.3	140	38.9	125	290072	40	-19.3	2500	0	273752	0	99789	-95926
10	21.7	5.4	140	26.1	125	87202	25	-29.8	2500	0	75702	0	62405	-43283
11	24.7	0.0	140	10.0	125	30754	32	-38.9	2500	0	23931	0	79325	-19317
											Summation:	214181	682612	831211

$$F = \frac{\Sigma[(W\cos\alpha)\tan\phi + c\Delta\ell]}{\Sigma W\sin\alpha} = \frac{214181 + 682612}{831211} = 1.08$$

Figure 7.13 Manual calculations for stability of cohesionless fill slope on saturated clay foundation using the Ordinary Method of Slices and the critical circular slip surface found using Spencer's procedure.

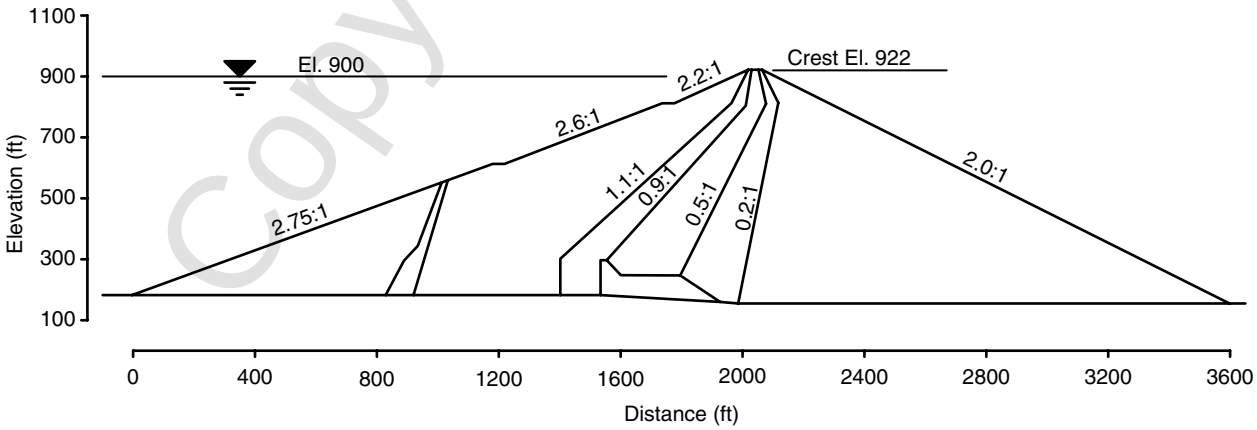


Figure 7.14 Cross section of Oroville Dam.

Copyrighted Material

Copyright © 2005 John Wiley & Sons Retrieved from: www.knovel.com

Table 7.6 Relationship Between the Ratio $\sigma'_{ff}/\sigma'_{3f}$ and the Friction Angle

ϕ' (deg)	$\frac{\sigma'_{ff}}{\sigma'_{3f}}$
30	1.50
40	1.64
50	1.77

normal stress, the confining pressure, σ'_{3f}, was computed assuming values of 1.5, 1.65, and 1.8 for the ratio $\sigma'_{ff}/\sigma'_{3f}$. The resulting confining pressures were then used to compute the friction angles from Eq. (7.34). The assumed value for the ratio, $\sigma'_{ff}/\sigma'_{3f}$, can be seen to have very little effect on the friction angle computed for a given confining pressure. The maximum difference between the friction angles computed assuming 1.5 and 1.8 for the ratio, $\sigma'_{ff}/\sigma'_{3f}$, was only 0.8°. The shear stress, τ_{ff}, defining the Mohr failure envelope for a given normal stress, σ'_{ff}, is computed by multiplying the normal stress by the tangent of the friction angle (i.e., $\tau_{ff} = \sigma'_{ff} \tan \phi'$). A 0.8° difference in the friction angle corresponds to a difference of no more than 3% in the shear stress. If it is assumed that the ratio, $\sigma'_{ff}/\sigma'_{3f}$, is 1.5 when the value may actually be somewhat higher, the resulting value for the friction angle will be estimated slightly conservatively.

Based on the preceding discussion, a nonlinear Mohr failure envelope was determined for the Oroville Dam shell material using values of $\phi_0 = 51°$ and $\Delta\phi = 6°$, and assuming that $\sigma'_{ff}/\sigma'_{3f} = 1.5$. The envelope was defined by a series of discrete points computed using the following steps:

1. A range in values of normal stress was established to encompass the maximum range expected for Oroville Dam. The minimum normal stress of interest was considered to be the normal stress at a depth of 1 ft, which for a total unit weight of 150 pcf was taken to be 150 psf. The maximum normal stress was estimated based on the height of the dam. For a height of 770 ft and a unit weight of 150 pcf, the maximum stress is approximately 115,000 psf.
2. Specific values of normal stress, σ', ranging from 150 psf to the maximum were selected for computing points defining the Mohr–Coulomb failure envelope. Beginning with the minimum stress of 150 psf, a geometric progression of values was used (e.g., 150, 300, 600, 1200 psf). Particular attention was paid to selecting points at low stresses because it was anticipated that the critical slip surface would be relatively shallow due to the cohesionless nature of the Oroville Dam shell material.
3. For each value of normal stress the corresponding value of the confining pressure was computed as

Table 7.8 Points Calculated to Define the Nonlinear Mohr Failure Envelope for the Oroville Dam Shell Material

σ'	σ'_3	ϕ'	τ
150	100	59.0	250
300	200	57.1	465
600	400	55.3	870
1,200	800	53.5	1,625
2,400	1,600	51.7	3,040
4,800	3,200	49.9	5,705
9,600	6,400	48.1	10,705
19,200	12,800	46.3	20,100
38,400	25,600	44.5	37,740
76,800	51,200	42.7	70,865
153,600	102,400	40.9	133,015

Table 7.7 Computed Secant Friction Angles for Different Confining Pressures and Various Assumed Values for the Ratio σ'_{ff}/σ'_3

	$\frac{\sigma'_{ff}}{\sigma'_{3f}} = 1.5$		$\frac{\sigma'_{ff}}{\sigma'_{3f}} = 1.65$		$\frac{\sigma'_{ff}}{\sigma'_{3f}} = 1.8$	
σ'_{ff} (psf)	σ'_3 (psf)	ϕ' (deg)	σ'_3 (psf)	ϕ' (deg)	σ'_3 (psf)	ϕ' (deg)
100	67	55.0	61	55.4	56	55.8
1,000	667	45.0	606	45.4	556	45.8
10,000	6,667	35.0	6,061	35.4	5556	35.8

Copyrighted Material

Copyright © 2005 John Wiley & Sons Retrieved from: www.knovel.com

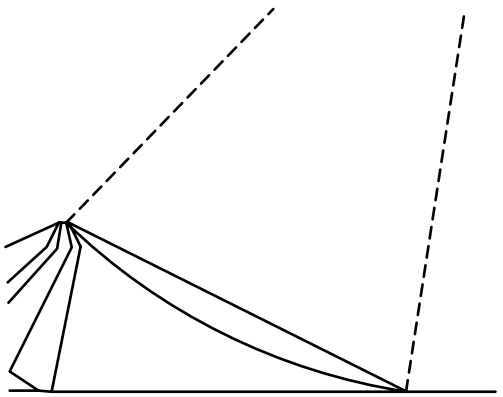


Figure 7.15 Critical circular slip surface for downstream slope of Oroville Dam.

$$\sigma_3' = \frac{\sigma'}{1.5} \tag{7.36}$$

4. Secant values of the friction angle were computed for each value of σ_3' from Eq. (7.34) as

$$\phi' = 51° - 6° \log_{10} \frac{\sigma_3'}{p_a} \tag{7.37}$$

where p_a (atmospheric pressure) is 2116 psf for units of pounds and feet that were used.

5. Shear stresses, τ, were calculated for each value of normal stress from

$$\tau = \sigma' \tan \phi' \tag{7.38}$$

The values calculated for the Oroville Dam shell material are summarized in Table 7.8. The pairs of values of σ' and τ were used as points defining a nonlinear Mohr failure envelope for the slope stability computations. Although not shown in this table, an additional point representing the origin ($\sigma' = 0$, $\tau = 0$) was included in the data defining the envelope for the slope stability computations. Nonlinear Mohr failure envelopes were also defined for the transition zone and the core of Oroville Dam; however, because the critical slip surface did not pass significantly through these zones, the shear strength data are not included here.

Slope stability computations. Slope stability computations were performed using the computer program and the nonlinear Mohr failure envelopes discussed earlier. Computations were performed using Spencer's procedure and circular slip surfaces. The critical slip surface is shown in Figure 7.15, and the minimum factor of safety is 2.28.

One way of checking the computer solution is to calculate the factor of safety manually using a procedure of slices such as the Ordinary Method of Slices or Simplified Bishop procedure. The friction angle could be varied for each slice depending on the normal stress, σ'. This is easiest to do with the Ordinary Method of Slices because the normal stress can be calculated independently of the shear strength using the following equation

$$\sigma' = \frac{W \cos \alpha - u\, \Delta l \cos^2 \alpha}{\Delta l} \tag{7.39}$$

With the Simplified Bishop procedure, the normal stress depends on the friction angle (i.e., the normal stress is part of the solution for the unknowns). Therefore, the normal stress must first be estimated to compute the friction angle, and then trial and error is used until the estimated and calculated values are in reasonable agreement. To estimate the friction angle initially for the Simplified Bishop procedure, either the normal stress can be estimated from the vertical overburden pressure or the normal stress can be calculated from Eq. (7.39) from the Ordinary Method of Slices.

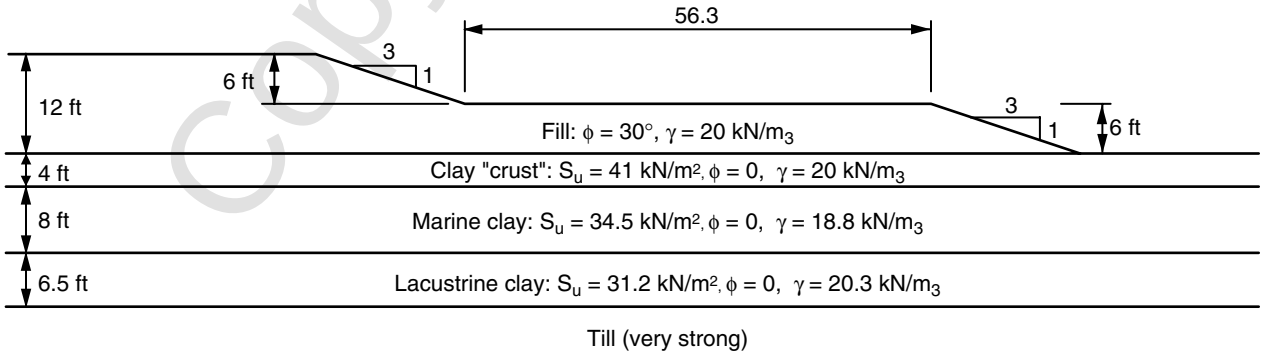


Figure 7.16 Cross section of James Bay dike.

Copyrighted Material

Copyright © 2005 John Wiley & Sons Retrieved from: www.knovel.com

Because the critical slip surface for the downstream slope was relatively shallow for this case, the infinite slope procedure was used to check the results of the computer solution. To do this the average normal stress was calculated for the critical slip surface found from the computer solution. The average normal stress was calculated using the equation

$$\sigma'_{av} = \frac{\sum \sigma_i \, \Delta l_i}{\sum \Delta l_i} \tag{7.40}$$

where the summations were performed for all slices. The average normal stress calculated for the critical slip surface was 12,375 psf. From the nonlinear Mohr failure envelope in Table 7.8, the corresponding shear stress, τ, is 13,421 psf and the equivalent secant friction angle is 47.3°. The factor of safety based on an infinite slope is then

$$F = \frac{\tan \phi'}{\tan \beta} = \frac{\tan 47.3°}{1/2.0} = 2.17 \tag{7.41}$$

This value (2.17) from the infinite slope analysis is within 5% of the value of 2.28 obtained from the computer solution with circular slip surfaces.

Recapitulation

- When the friction angle depends on the confining stress, the friction angle is expressed conveniently by a secant angle, which is a function of confining pressure, σ_3. This requires additional steps to determine an equivalent nonlinear Mohr failure envelope for slope stability analyses.
- To relate confining pressure, σ_3, to normal stress, σ, for a nonlinear Mohr failure envelope, the confining pressure can be assumed to be equal to two-thirds (= 1/1.5) the normal stress. This facilitates defining points on the Mohr failure envelope when the friction angle is defined in terms of confining pressure, σ_3.
- For shallow slides in cohesionless soils, stability computations can be checked with an infinite slope analysis, even when the Mohr failure envelope is nonlinear. When the Mohr failure envelope is nonlinear, the average normal stress on the slip surface from a computer solution can be used to define an equivalent secant friction angle that is then used in the infinite slope analysis.

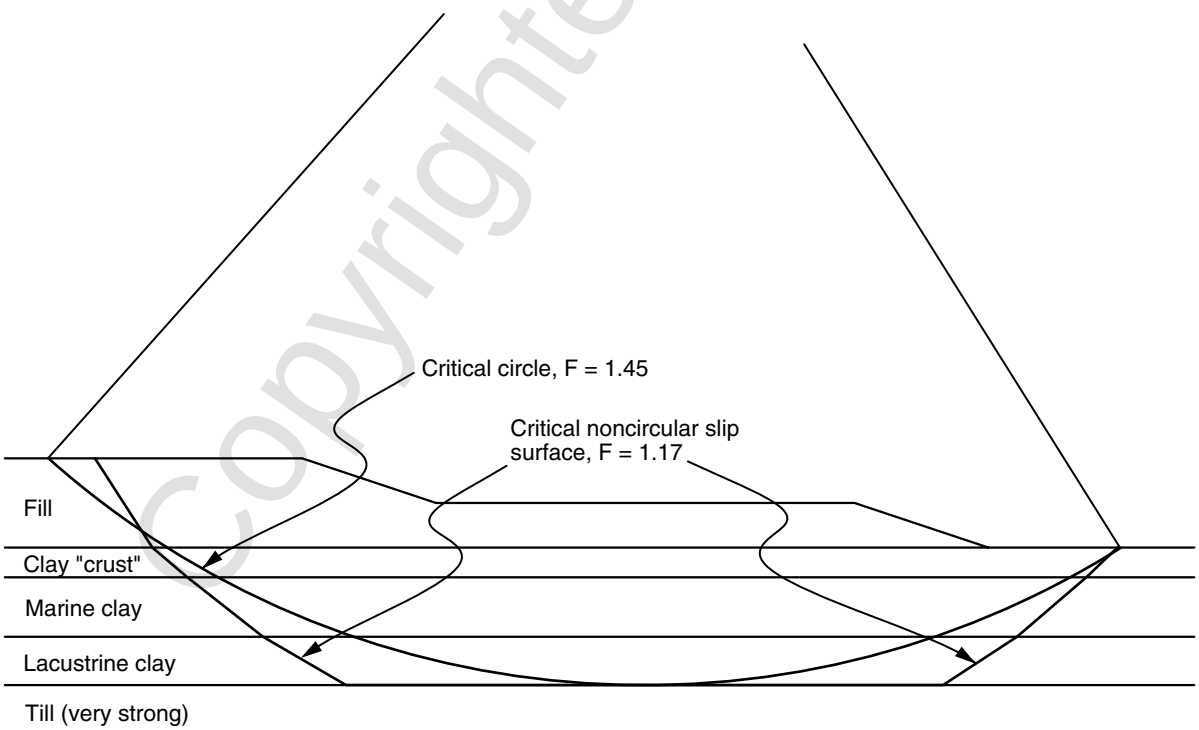


Figure 7.17 Critical circular and noncircular slip surfaces for James Bay dike.

Copyrighted Material

Copyright © 2005 John Wiley & Sons Retrieved from: www.knovel.com

Example 6: James Bay Dike

The James Bay hydroelectric project involved the design of dikes that were to be constructed on soft and sensitive clays (Christian et al., 1994). A typical cross section of one of the planned dikes is shown in Figure 7.16. Soil properties for the materials in the dike and its foundation are summarized in this figure.

An analysis was first performed using circular slip surfaces, with a computer program and Spencer's procedure. The minimum factor of safety was calculated to be 1.45 for the critical circle, which is shown in Figure 7.17. This value of 1.45 for the factor of safety is the same as the value (1.453) that Christian et al. reported for the slope.

Additional analyses were performed using noncircular slip surfaces and an automatic search. The automatic search was started with the critical circle from the previous analyses. Ten points were used to define the slip surface. These points were shifted systematically using the search routine implemented in the computer program until a minimum factor of safety was found. The corresponding critical noncircular slip surface was then adjusted by adding some points and removing others. Points were adjusted so that there was a point located at the interfaces between soil layers, and these points were shifted in the horizontal direction until the minimum factor of safety was again found. The most critical noncircular slip surface found after searching is shown in Figure 7.17. The corresponding minimum factor of safety is 1.17, which is approximately 20% less than the minimum value computed using circles.

Christian et al. (1994) discussed the effects of variations and uncertainties in shear strength on the computed factors of safety for the James Bay dikes. They showed that the variation in shear strength could have an important effect on the evaluation of stability. The results presented in the preceding paragraph show that the effect of using noncircular slip surfaces is of comparable magnitude, thus illustrating the importance of locating the critical slip surface accurately.

To verify the computations with noncircular slip surfaces, additional computations were performed using a force equilibrium procedure and a computer spreadsheet program. For these computations the interslice forces were assumed to be parallel; the interslice force inclination was assumed to be the same as the inclination (2.7 degrees) determined from the computer solution with Spencer's procedure. The spreadsheet computations are presented in Figure 7.18. The computed factor of safety was 1.17, thus verifying the value calculated using the computer program.

Recapitulation

- Noncircular slip surfaces may give significantly lower factors of safety than circles.
- The critical circle provides a good starting point for searching for the critical noncircular slip surface.
- A force equilibrium solution using a spreadsheet with the interslice force inclination from Spencer's procedure provides a good method for checking a computer solution with Spencer's procedure and is applicable to circular and noncircular slip surfaces.

Example 7: Homogeneous Earth Dam with Steady-State Seepage

A homogeneous earth embankment resting on a relatively impervious foundation is illustrated in Figure 7.19. The embankment impounds water on one side, and steady-state seepage is assumed to have developed. Stability computations were performed for this embankment to evaluate the long-term stability of the downstream slope. Drained effective stress shear strength parameters were used and are shown on the cross section of the embankment.

Pore water pressures. Finite element seepage analysis was performed for the embankment to calculate pore water pressures. The GMS/SEEP2D software was used for this purpose (Tracy, 1991; EMRL, 2001). The entire cross section of the embankment was modeled with finite elements, and appropriate saturated or unsaturated hydraulic conductivities were assigned depending on the pore water pressure. The hydraulic conductivity for the saturated soil (positive pressures) was 1×10^{-5} ft/min. The hydraulic conductivity for the unsaturated soil was assumed to decrease sharply to a residual hydraulic conductivity equal to 0.1% of the value for saturated conditions as the water pressures decreased below atmospheric. This essentially restricted almost all flow to the saturated (positive water pressure) zone of the cross section. The finite element mesh used for this problem contained 589 node points and 1044 elements.

Finite element seepage analyses produced values of pore water pressure at each node point. These values of pore water pressure were then used to interpolate values of pore water pressure along each slip surface in the slope stability computations. Interpolation was performed using the triangle-based interpolation scheme described by Wright (2002). This scheme is very efficient and introduces negligible error caused by

Copyrighted Material

Copyright © 2005 John Wiley & Sons Retrieved from: www.knovel.com

Computation of slice weights

Slice No.	b	h_1	γ_1	h_2	γ_2	h_3	γ_3	h_4	γ_4	W
1	7.7	6.0	20	-	20	-	18.8	-	20.3	926
2	4.7	12.0	20	2.0	20	-	18.8	-	20.3	1319
3	10.2	12.0	20	4.0	20	4.0	18.8	-	20.3	4019
4	11.2	11.5	20	4.0	20	8.0	18.8	3.2	20.3	5868
5	12.1	8.0	20	4.0	20	8.0	18.8	6.5	20.3	6333
6	28.2	6.0	20	4.0	20	8.0	18.8	6.5	20.3	13572
7	28.2	6.0	20	4.0	20	8.0	18.8	6.5	20.3	13572
8	11.9	4.0	20	4.0	20	8.0	18.8	6.5	20.3	5270
9	9.9	0.6	20	4.0	20	8.0	18.8	3.2	20.3	3064
10	9.3	-	20	4.0	20	4.0	18.8	-	20.3	1446
11	4.2	-	20	2.0	20	-	18.8	-	20.3	168

Computation of factor of safety

Slice No.	W	α	$\Delta\ell$	c	ϕ	u	W sinα	$-c\Delta\ell - (W\cos\alpha - u\Delta\ell)\tan\phi'$	$F_1 = 1.0$		$F_2 = 1.2$		$F_3 = 1.4$	
									n_α	Z_{i+1}	n_α	Z_{i+1}	n_α	Z_{i+1}
1	926	57.2	14.3	0.0	30	0	779	-289	1.050	466	0.972	554	0.916	625
2	1319	40.3	6.2	41.0	0	0	854	-253	0.791	1225	0.791	1366	0.791	1475
3	4019	38.2	12.9	34.5	0	0	2485	-446	0.814	3730	0.814	3962	0.814	4137
4	5868	30.2	12.9	31.5	0	0	2952	-406	0.887	6601	0.887	6909	0.887	7139
5	6333	0.0	12.1	31.5	0	0	0	-382	0.999	6218	0.999	6591	0.999	6866
6	13572	0.0	28.2	31.5	0	0	0	-887	0.999	5331	0.999	5851	0.999	6232
7	13572	0.0	28.2	31.5	0	0	0	-887	0.999	4453	0.999	5111	0.999	5597
8	5270	0.0	11.9	31.5	0	0	0	-375	0.999	4068	0.999	4798	0.999	5329
9	3064	-33.1	11.9	31.5	0	0	-1675	-374	0.811	1541	0.811	2348	0.811	2934
10	1446	-40.6	12.3	34.5	0	0	-942	-424	0.728	-336	0.728	569	0.728	1224
11	168	-43.7	5.8	41	0	0	-116	-238	0.690	**-847**	0.690	**114**	0.690	**811**

$$Z_{i+1} = Z_i + \frac{W\sin\alpha - \dfrac{c\Delta\ell + (W\cos\alpha - c\Delta\ell)\tan\phi'}{F}}{n_\alpha}$$

$$n_\alpha = \cos(\alpha - \theta) + \frac{\sin(\alpha - \theta)\tan\phi'}{F}$$

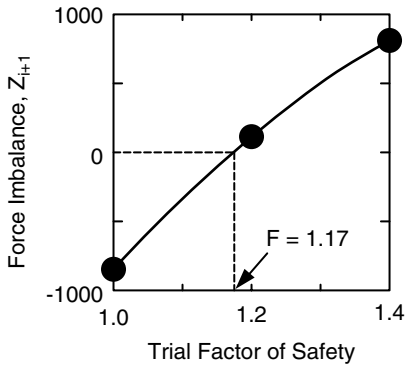


Figure 7.18 Manual calculations for James Bay dike using force equilibrium procedure.

Copyrighted Material

Copyright © 2005 John Wiley & Sons Retrieved from: www.knovel.com

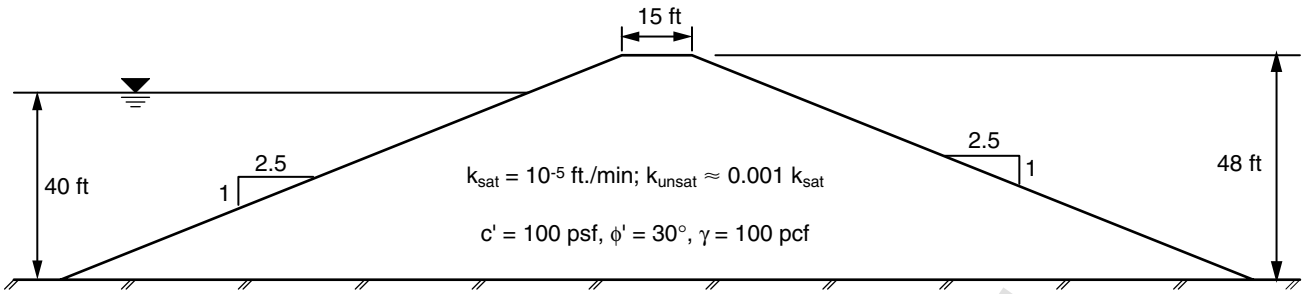


Figure 7.19 Cross section for homogeneous embankment with steady-state seepage.

interpolation. In fact, many fewer nodes and elements could probably have been used for the finite element seepage analysis with no loss in accuracy in the computed factor of safety (Wright, 2002).

The finite element seepage analysis was also used to determine a position for a phreatic surface and a piezometric line (Figure 7.20). The phreatic surface and piezometric line were assumed to be the same as the line of zero pore water pressure determined from contours of pore water pressure obtained from the finite element seepage analysis. Experience with a number of finite element seepage analyses where both saturated and unsaturated flow has been modeled has shown that the contour of zero pore water pressure corresponds very closely to the classical line of seepage described by Casagrande (1937) for saturated flow.

For the slope stability computations, pore water pressures were calculated from the phreatic surface and piezometric line using the procedures discussed in Chapter 6. The pore water pressures calculated from the phreatic surface were always as small as or smaller than those based on the piezometric line and were usually slightly larger than those based on the actual finite element seepage analysis.

Although the pore water pressures calculated in the finite element analyses were negative in the uppermost part of the flow region, above the piezometric line and phreatic surface, negative pore water pressures were neglected in all of the slope stability calculations. Negative pore water pressures probably would exist and would contribute slightly to stability, but their effect would be small for this problem and it seems reasonable to neglect them. Only when negative pore water pressures can be sustained throughout the life of the slope should they be counted on for stability. Sustainable negative pore water pressures seem unlikely for most slopes.

Stability analyses. Slope stability calculations were first performed using a computer program and each of the three representations of pore water pressure discussed above. Spencer's procedure was used for all of the calculations. In each case an automatic search was conducted to locate the most critical circle for each representation of pore water pressures. The minimum factors of safety are summarized in Table 7.9. All three

Table 7.9 Summary of Factors of Safety from Slope Stability Computations for Homogeneous Embankment Subjected to Steady-State Seepage (Spencer's Procedure and Circular Clip Surfaces)

Procedure of slices	Factor of safety
Finite element seepage analysis—pore water pressures interpolated	1.19
Piezometric line	1.16
Phreatic surface	1.24

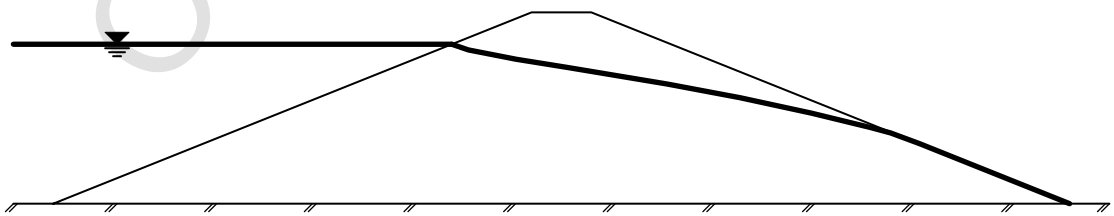


Figure 7.20 Zero-pressure line (contour) used as phreatic surface and piezometric line for homogeneous embankment.

Copyrighted Material

Copyright © 2005 John Wiley & Sons Retrieved from: www.knovel.com

representations of pore water pressure produced similar values for the factor of safety, with the differences between the rigorous finite element solution and the approximate representations being 4% or less. As expected, the piezometric line produced lower factors of safety than the phreatic surface, although the differences were small. The phreatic surface did, however, result in a higher factor of safety than the rigorous finite element solution, and thus this approximation errs on the unsafe side for these conditions.

A manual solution using a computer spreadsheet program and the Ordinary Method of Slices was performed as verification of the computer solutions. Calculations were performed using both the preferred and alternative methods of handling pore water pressures in the Ordinary Method of Slices that were discussed in Chapter 6. For both sets of calculations the pore water pressures were calculated using the piezometric line.

The calculations for the Ordinary Method of Slices are presented in Figures 7.21 and 7.22 for the preferred and alternative methods, respectively. Using the preferred method of handling pore water pressures, the factor of safety was 1.19 (Figure 7.21). This value is identical to the value calculated using the finite element seepage solution and slightly higher than the value with the piezometric line based on the computer solutions with Spencer's procedure. The other, alternative method of handling pore water pressures in the Ordinary Method of Slices resulted in a lower factor of safety of 1.08, which is approximately 10% lower than the other solutions. This is consistent with what was shown in Chapter 6 for the Ordinary Method of Slices and illustrates why the form of the method illustrated in Figure 7.21 is preferred.

The final set of calculations was performed using the charts in the Appendix and are summarized in Figure 7.23. The factor of safety from the chart solution is 1.08. This value is slightly lower than the values from the more accurate computer solutions. The slightly lower value from the chart solution probably reflects use of the Ordinary Method of Slices to develop the charts as well as other approximations that are made regarding seepage and pore water pressures.

Slice No.	b (ft)	h_{soil} (ft)	γ_{soil} (pcf)	W (lb)	$\Delta\ell$	α (deg)	c' (psf)	ϕ (deg)	$h_{piezometric}$(1)	$u^{(2)}$ (psf)	$u\Delta\ell\cos^2\alpha$	W cosα	W cosα - $u\Delta\ell\cos^2\alpha$	(W cosα – $u\Delta\ell\cos^2\alpha$)tanϕ'	c'$\Delta\ell$	W sinα
1	7.3	2.6	125	2392	11.0	48.1	100	30	0.0	0	0	1597	1597	922	1096	1780
2	11.1	7.6	125	10580	14.4	39.8	100	30	3.4	213	1818	8128	6310	3643	1443	6772
3	7.3	10.9	125	9866	8.6	32.2	100	30	8.2	515	3160	8345	5185	2994	858	5264
4	7.5	12.1	125	11383	8.4	26.7	100	30	10.6	663	4462	10174	5711	3297	843	5107
5	5.1	12.5	125	7886	5.5	22.1	100	30	11.9	745	3488	7307	3819	2205	545	2966
6	7.3	12.2	125	11153	7.7	17.8	100	30	12.1	756	5253	10617	5364	3097	767	3418
7	11.6	10.8	125	15671	11.9	11.4	100	30	10.8	673	7669	15360	7691	4440	1186	3106
8	11.5	7.7	125	11098	11.5	3.8	100	30	7.7	482	5529	11073	5545	3201	1153	732
9	12.3	2.9	125	4466	12.4	-4.0	100	30	2.9	181	2225	4455	2230	1287	1235	-315
													Summation:	25087	9126	28832

(1) $h_{piezometric}$ = depth below piezometric line to slip surface.
(2) $u = \gamma_w \times h_{piezometric}$

$$F = \frac{\Sigma[(W\cos\alpha - u\Delta\ell\cos^2\alpha)\tan\phi - c\Delta\ell]}{\Sigma W\sin\alpha} = \frac{25087 + 9126}{28832} = 1.19$$

Figure 7.21 Manual calculations for stability of embankment with steady-state seepage using the Ordinary Method of Slices (the preferred method of representing pore water pressures).

Copyrighted Material

Copyright © 2005 John Wiley & Sons Retrieved from: www.knovel.com

Slice No.	b (ft)	h_{soil} (ft)	γ_{soil} (pcf)	W (lb)	$\Delta\ell$	α (deg)	c' (psf)	ϕ (deg)	$h_{piezometric}$(1)	$u^{(2)}$ (psf)	u $\Delta\ell$	W cosα	W cosα - u $\Delta\ell$	(W cosα – u $\Delta\ell$) tanϕ'	c'$\Delta\ell$	W sinα
1	7.3	2.6	125	2392	11.0	48.1	100	30	0.0	0	0	1597	1597	922	1096	1780
2	11.1	7.6	125	10580	14.4	39.8	100	30	3.4	213	3080	8128	5048	2915	1443	6772
3	7.3	10.9	125	9866	8.6	32.2	100	30	8.2	515	4417	8345	3928	2268	858	5264
4	7.5	12.1	125	11383	8.4	26.7	100	30	10.6	663	5587	10174	4587	2648	843	5107
5	5.1	12.5	125	7886	5.5	22.1	100	30	11.9	745	4062	7307	3245	1873	545	2966
6	7.3	12.2	125	11153	7.7	17.8	100	30	12.1	756	5798	10617	4819	2782	767	3418
7	11.6	10.8	125	15671	11.9	11.4	100	30	10.8	673	7983	15360	7377	4259	1186	3106
8	11.5	7.7	125	11098	11.5	3.8	100	30	7.7	482	5553	11073	5521	3187	1153	732
9	12.3	2.9	125	4466	12.4	-4.0	100	30	2.9	181	2236	4455	2219	1281	1235	-315
													Summation:	22136	9126	28832

(1) $h_{piezometric}$ = depth below piezometric line to slip surface.
(2) $u = \gamma_w \times h_{piezometric}$

$$F = \frac{\Sigma[(W\cos\alpha - u\Delta\ell\cos^2\alpha)\tan\phi - c\Delta\ell]}{\Sigma W\sin\alpha} = \frac{22136 + 9126}{28832} = 1.08$$

Figure 7.22 Manual calculations for stability of embankment with steady-state seepage using the Ordinary Method of Slices (a poor method of representing pore water pressures).

Nevertheless, the chart solution confirms the validity of the other more accurate solutions for this example and is conservative.

Recapitulation

- The zero-pressure line from finite element seepage analysis can be used to define an equivalent piezometric line and phreatic surface.
- Pore water pressures determined by interpolation of pressures from finite element seepage analysis and pore water pressures represented by an equivalent piezometric line and a phreatic surface all produced similar factors of safety, with pore water pressures from a piezometric line producing the lowest factors of safety.
- The form of the Ordinary Method of Slices recommended for effective stress analyses in Chapter 6 produces much better agreement with complete equilibrium procedures than the alternative form.

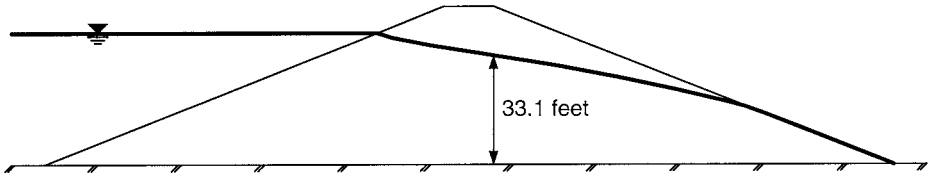
Example 8: Earth Dam with Thick Core—Steady-State Seepage

A series of stability computations similar to those for the preceding example was performed for the earth dam shown in Figure 7.24. Soil properties for the core and shell of the dam are shown in the figure. The primary purposes of this example were to illustrate with additional computations the differences among various methods for representing pore water pressures in a slope stability analysis and to present results of a spreadsheet solution using the Simplified Bishop procedure for effective stress analyses.

Pore water pressures were calculated from a finite element analysis with GMS/SEEP2D software. A piezometric line and phreatic surface were determined from the finite element analysis by locating the zero-pressure line as described for the preceding example. Slope stability computations were performed for the three representations of pore water pressure using the computer program and Spencer's procedure with circular slip surfaces. Results of these calculations are

Copyrighted Material

Copyright © 2005 John Wiley & Sons Retrieved from: www.knovel.com



STEP 1: Calculation of P_d:

$\beta = \text{atan}(1/2.5) = 21.8°$

$\gamma = 100$ pcf

$H = 48$ ft

$q = 0$

$H_w = 0$

$\mu_q = \mu_w = \mu_t = 1.0$

$$P_d = \frac{\gamma H + q - \gamma_w H_w}{\mu_q \mu_w \mu_t}$$

$$P_d = \frac{(100)(48)}{(1)(1)(1)} = 4800 \text{ psf}$$

STEP 2: Calculation of P_e:

$H_c = 33.1$ feet (see figure above)

$H_c/H = (33.1)/(48) = 0.69$

$H'_w/H = 0.76$ (from Fig. A-6)

$\mu'_w = 0.97$ (from Fig. A-3)

$H'_w = (0.76)(48) = 36.5$ ft

$$P_e = \frac{\gamma H + q - \gamma_w H_w'}{\mu_q \mu_w'}$$

$$P_e = \frac{(100)(48) - (62.4)(36.5)}{(1.0)(0.97)} = 2600 \text{ psf}$$

STEP 3: Calculation of $\lambda_{c\phi}$:

$\phi' = 30°$

$c' = 100$ psf

$$\lambda_{c\phi} = \frac{P_e \tan\phi'}{c}$$

$$\lambda_{c\phi} = \frac{(2600)\tan(30)}{100} = 15$$

STEP 4: Determination of N_{cf}:

$N_{cf} = 52$ (from Fig. A-5; $\cot\beta = 2.5$, $\lambda_{c\phi} = 15$)

STEP 5: Computation of F:

$$F = N_{cf}\frac{c}{P_d} = 52\frac{100}{4800} = 1.08$$

Figure 7.23 Calculations for stability of homogeneous embankment with steady-state seepage using Janbu's slope stability charts.

Material Properties			
Zone	c' - psf	ϕ' - deg	k - ft/min
Core	0	20	1×10^{-5}
Shell	0	38	1×10^{-3}

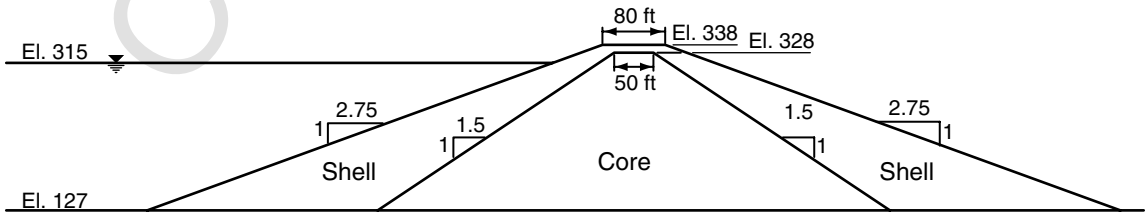


Figure 7.24 Cross section and soil properties for earth dam with thick clay core.

Copyrighted Material

Copyright © 2005 John Wiley & Sons Retrieved from: www.knovel.com

summarized in Table 7.10. The results shown in this table are very similar to those shown for the homogeneous dam in the preceding example: The piezometric line produces a slightly lower factor of safety that the more rigorous interpolation of pore water pressures, while the phreatic surface approximation produces a slightly higher value for the factor of safety. All three representations in this case produce very similar values for the factor of safety.

Additional computations were performed using the computer program with the Simplified Bishop procedure and the piezometric line to represent pore water pressures. The factor of safety calculated by the Simplified Bishop procedure was 1.61, which is approximately 4% less than the corresponding value (1.67) by Spencer's procedure. One of the purposes of calculating the factor of safety by the Simplified Bishop procedure was to be able to compare the value from the computer solution with a manual solution using a spreadsheet. Results of the spreadsheet solution for the critical circle found with the Simplified Bishop procedure are summarized in Figure 7.25. The factor of safety calculated by the spreadsheet solution (1.61) is the same as the value calculated with the computer program.

Recapitulation

- Conclusions similar to those reached for the homogeneous dam can be drawn regarding the representations of pore water pressures: All three representations of pore water pressure produced similar results, with the piezometric line producing the lowest factors of safety.
- The Simplified Bishop procedure provides an excellent check of a computer solution for effective stress analyses with circular slip surfaces.

Example 9: Reinforced Slope (1)

This and the next example were selected to demonstrate how results obtained using one computer program may be verified using another computer program. The two examples chosen are part of the user's documentation for the STABGM 2.0 slope stability software (Duncan et al., 1998). The first example involves an embankment resting on a soft, saturated clay foundation with a single layer of reinforcement at the base of the embankment (Figure 7.26). Because the clay in the foundation will consolidate with time and become stronger under the weight of the overlying embankment, the short-term stability condition is most critical and was selected for analyses. The undrained shear strength profile for the foundation is shown along with the other soil properties in Figure 7.26.

Stability computations were performed with the UTEXAS4 computer program using the Simplified Bishop procedure. An automatic search was conducted to find the most critical slip surface, giving a minimum factor of safety of 1.13. This value is approximately 5% less than the value of 1.19 that is reported in the STABGM user's documentation. Differences of this magnitude (5%) are larger than normally expected when two different computer programs are used, provided that both programs use the same input data and the same procedures for computation. In the present case the relatively large difference is due to differences in the degree of refinement of the search used to locate a critical slip surface. The critical circle reported using STABGM is shown in Figure 7.27 along with the critical circle found using UTEXAS4. With STABGM, circles were only investigated at depths corresponding to the bottom of each soil layer shown in Figure 7.27. With UTEXAS4, circles were also investigated at intermediate depths, and a more critical circle was found. STABGM would probably have given the same factor of safety as UTEXAS4 had a more refined search been used in the STABGM analyses.

An additional set of stability calculations was performed with UTEXAS4 for the critical circle from STABGM. The computed factor of safety for this circle with UTEXAS4 was 1.19, which is identical to the value reported by STABGM. This confirms that the differences in factor of safety reported earlier were due to the input data for the automatic search rather than to differences between the two programs. The close agreement in results when comparable conditions are used verifies the correctness of the results for this case.

Table 7.10 Summary of Slope Stability Calculations for Dam with Clay Core (Spencer's Procedure and Circular Clip Surfaces)

Procedure of slices	Factor of safety
Finite element seepage analysis—pore water pressures interpolated	1.69
Piezometric line	1.67
Phreatic surface	1.70

Recapitulation

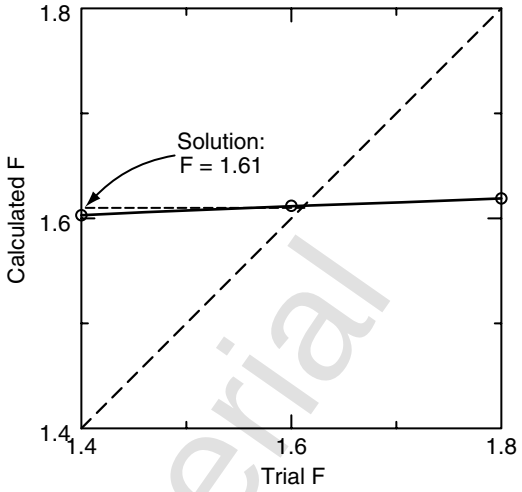
- One computer program may be used to verify results obtained by another computer program.
- When comparing results from two different computer programs, it is important to compare results for the same conditions, including the same slope geometry, soil properties, and slip surface.

Copyrighted Material

Copyright © 2005 John Wiley & Sons Retrieved from: www.knovel.com

Slice No.	b (ft)	h_{shell} (ft)	γ_{shell} (pcf)	h_{core} (ft)	γ_{core} (pcf)	W (lb)
1	20.0	13.1	140	0.0	120	36659
2	35.2	20.8	140	26.6	120	215174
3	65.0	10.0	140	76.0	120	683527
4	62.5	29.5	140	84.9	120	894190
5	89.9	52.5	140	69.1	120	1406585
6	105.7	82.2	140	34.2	120	1648280
7	21.2	101.4	140	5.6	120	315386
8	81.8	92.2	140	0.0	120	1055716
9	114.7	54.1	140	0.0	120	867907
10	49.8	14.2	140	0.0	120	98993

(*a*)



(*c*)

Slice No.	W (lbs)	α (degs)	W sinα	c' (psf)	φ' (degs)	$h_{piezometric(1)}$	$u^{(2)}$ (psf)	cb + (W – ub) tanφ'	Trial F = 1.4		Trial F = 1.6		Trial F = 1.8	
									m_α	[cb + (W - ub) tanφ'] ÷ m_α	m_α	[cb + (W - ub) tanφ'] ÷ m_α	m_α	[cb + (W - ub) tanφ'] ÷ m_α
1	36659	43.2	25110	0	38	0.0	0	28641	1.11	28641	1.06	26942	1.03	27918
2	215174	40.2	138831	0	20	23.2	1450	59724	0.93	59724	0.91	65575	0.89	666770
3	683527	35.0	391572	0	20	38.3	2392	192187	0.97	192187	0.95	202309	0.94	205441
4	894190	28.7	429214	0	20	55.3	3449	247055	1.00	247055	0.99	250447	0.97	253565
5	1406585	21.7	519784	0	20	59.9	3741	389600	1.03	389600	1.01	384494	1.00	388071
6	1648280	13.1	374514	0	20	34.2	2131	517970	1.03	517970	1.03	505074	1.02	507919
7	315386	7.7	42435	0	20	11.5	719	109240	1.03	109240	1.02	106939	1.02	107296
8	1055716	3.4	62854	0	38	12.9	805	773349	1.03	773349	1.03	752799	1.02	755174
9	867907	-4.8	-72569	0	38	7.2	452	637567	0.95	671239	0.96	667142	0.96	663990
10	98993	-11.7	-20099	0	38	0.0	0	77342	0.87	77342	0.88	87886	0.89	86799
		Sum:	1891646						Sum:	3033119	Sum:	3049608	Sum:	3062944

(1) $h_{piezometric}$ = depth below piezometric line to slip surface.

(2) $u = \gamma_w \times h_{piezometric}$

$$F = \frac{\sum \left[\frac{c'b + (W - ub)\tan\phi}{m_\alpha} \right]}{\sum W \sin\alpha}$$

$$m_\alpha = \cos\alpha + \frac{\sin\alpha + \tan\phi}{F}$$

$$F_1 = \frac{3033119}{1891646} = 1.603 \qquad F_2 = \frac{3049608}{1891646} = 1.612 \qquad F_3 = \frac{3062944}{1891646} = 1.619$$

(*b*)

Figure 7.25 Manual calculations for stability of clay core dam with steady-state seepage using the Simplified Bishop procedure: (*a*) calculation of slice weights; (*b*) calculations for factor of safety; (*c*) summary of trial-and-error solution for *F*.

Copyrighted Material

Copyright © 2005 John Wiley & Sons Retrieved from: www.knovel.com

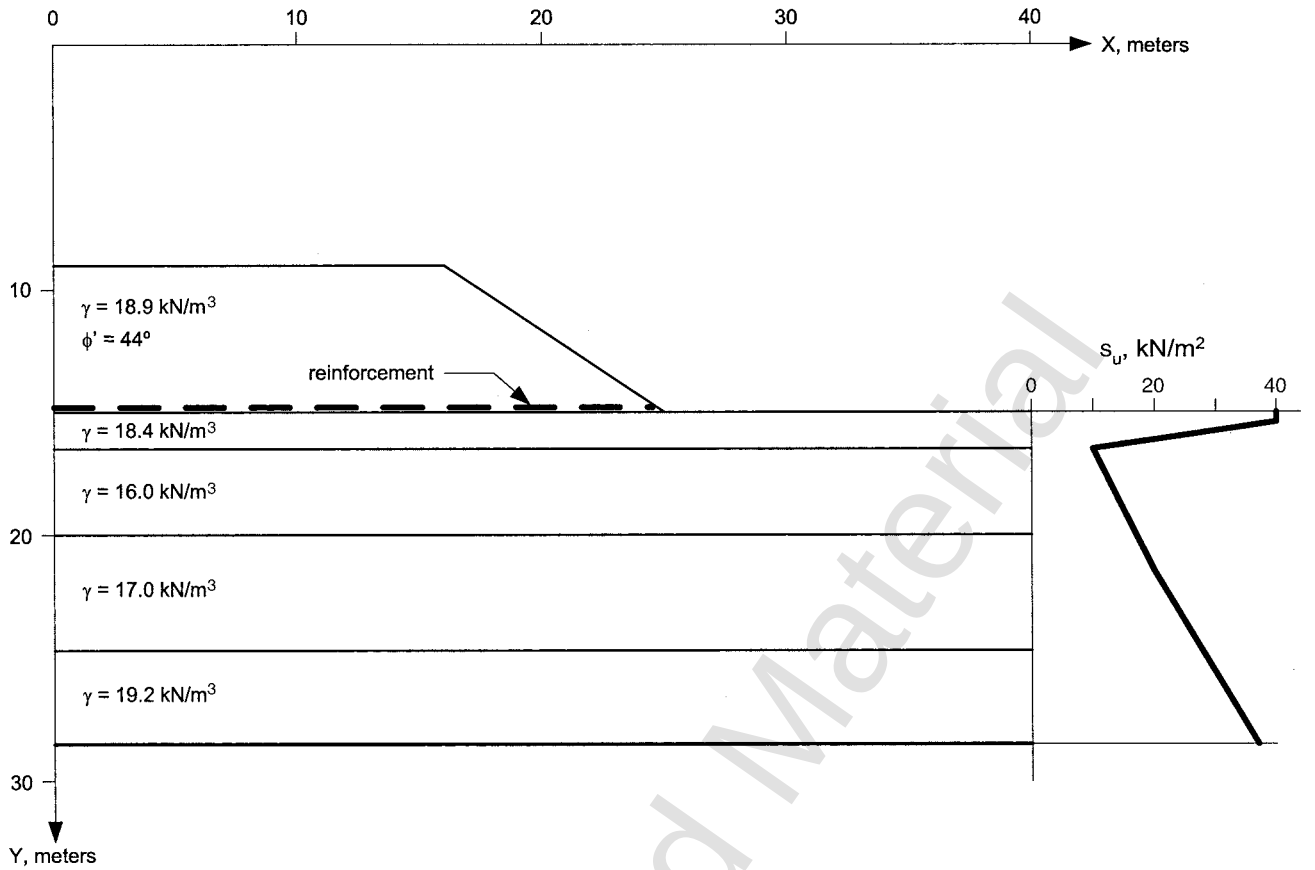


Figure 7.26 Soil properties and slope geometry for reinforced embankment on a soft clay foundation from the STABGM user's documentation.

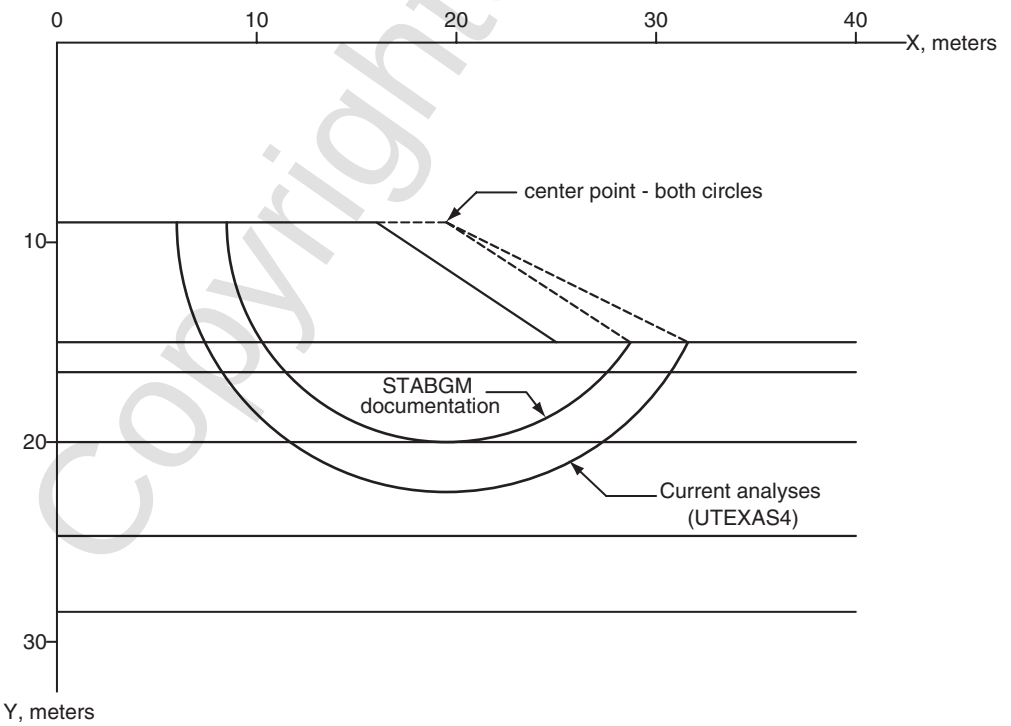
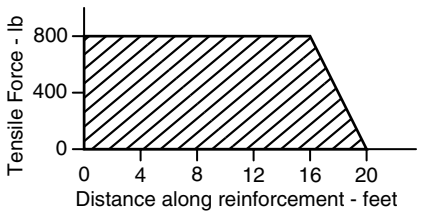


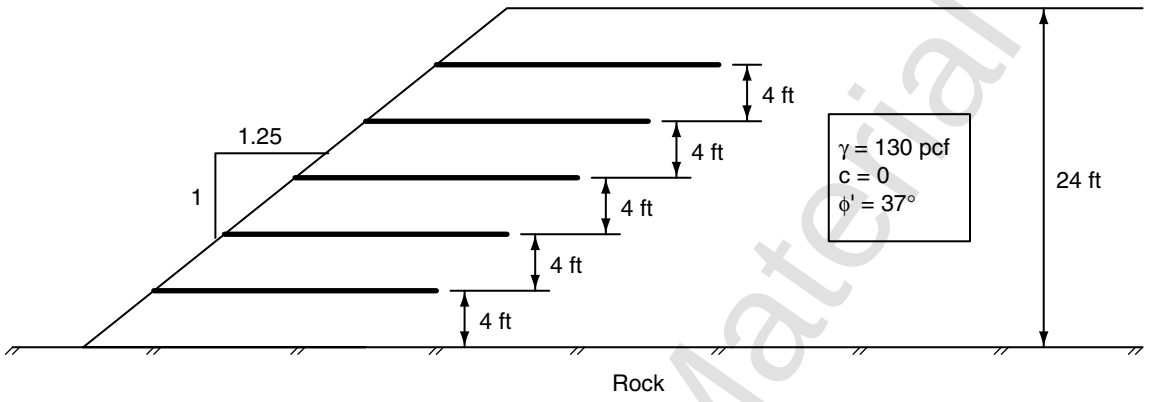
Figure 7.27 Critical circles for reinforced embankment on a soft clay foundation.

Copyrighted Material

Copyright © 2005 John Wiley & Sons Retrieved from: www.knovel.com



(*a*)



(*b*)

Figure 7.28 Reinforced slope on a rock foundation foundation from the STABGM user's documentation: (*a*) distribution of longitudinal forces along each reinforcing element; (*b*) slope and reinforcement geometry with soil properties.

Copyrighted Material

Example 10: Reinforced Slope (2)

This example is for a reinforced fill slope resting on a much stronger soil foundation and is also described in the STABGM 2.0 user's manual (Duncan et al., 1998). The slope and soil properties are presented in Figure 7.28. The soil in the slope is assumed to drain freely, and thus long-term stability computations were performed using shear strengths expressed in terms of effective stresses. The slope contains six layers of reinforcement, beginning at the bottom of the slope and spaced 4 ft apart vertically. Each reinforcement layer is 20 ft long, with a tensile force of 800 lbs per lineal foot, decreasing linearly to zero over the final 4 ft of embedded length.

Slope stability analyses were performed using UTEXAS4 with circular slip surfaces and Spencer's procedure. The minimum factor of safety calculated was 1.61. This value is less that the value of 1.71 that is reported by Duncan et al. using STABGM 2.0, representing a difference of approximately 6% in the factor of safety. As discussed for the preceding example, differences of this magnitude (5 to 6%) are larger than expected for two computer programs if the same con-

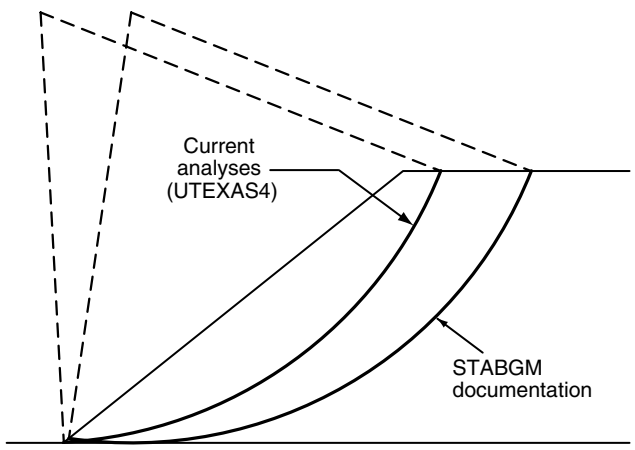


Figure 7.29 Critical circles for reinforced slope on rock foundation.

Copyright © 2005 John Wiley & Sons Retrieved from: www.knovel.com

ditions are analyzed. Subsequently, an analysis was performed using UTEXAS4 and the critical circle that was found using SSTABGM 2.0. The factor of safety was then calculated to be 1.71, which is identical to the value reported by Duncan et al. for the critical circle found using STABGM. The critical circles found using UTEXAS4 and STABGM 2.0 are plotted in Figure 7.29. It can be seen that the two circles are different. If a more refined search had been conducted with STABGM 2.0, it is likely that the minimum factor of safety would have been similar to the minimum factor of safety (1.61) found with UTEXAS4.

Copyrighted Material

Copyright © 2005 John Wiley & Sons Retrieved from: www.knovel.com